

Predictability of Midsummer Great Plains Low-Level Jet and Associated Precipitation

KELSEY M. MALLOY AND BEN P. KIRTMAN

Rosenstiel School of Marine and Atmospheric Science, University of Miami, Miami, Florida

(Manuscript received 15 May 2019, in final form 6 November 2019)

ABSTRACT

Warm-season precipitation in the U.S. “Corn Belt,” the Great Plains, and the Midwest greatly influences agricultural production and is subject to high interannual and intraseasonal variability. Unfortunately, current seasonal and subseasonal forecasts for summer precipitation have relatively low skill. Therefore, there are ongoing efforts to understand hydroclimate variability targeted at improving predictions, particularly through its primary transporter of moisture: the Great Plains low-level jet (LLJ). This study uses the Community Climate System Model, version 4 (CCSM4), July forecasts, made as part of the North American Multi-Model Ensemble (NMME), to assess skill in reproducing the monthly Great Plains LLJ and associated precipitation. Generally, the CCSM4 forecasts capture the climatological jet but have problems representing the observed variability beyond two weeks. In addition, there are predictors associated with the large-scale variability identified through linear regression analysis, shifts in kernel density estimators, and case study analysis that suggest potential for improving confidence in forecasts. In this study, a strengthened Caribbean LLJ, negative Pacific–North American (PNA) teleconnection, El Niño, and a negative Atlantic multidecadal oscillation each have a relatively strong and consistent relationship with a strengthened Great Plains LLJ. The circulation predictors, the Caribbean LLJ and PNA, present the greatest “forecast of opportunity” for considering and assigning confidence in monthly forecasts.


1. Introduction

Warm-season extreme precipitation in the north-central Great Plains has significant socioeconomic implications, ranging from agricultural production to human and property loss from associated flooding. For this reason, there are ongoing efforts to understand Great Plains hydroclimate variability and improve both seasonal and subseasonal prediction of heavy rainfall events as well as how a lack of such events might lead to drought.

Extreme warm-season precipitation in the United States dominates in the north-central and Midwest regions (Dirmeyer and Kinter 2010), and the leading cause is the strengthening of the Great Plains low-level jet (LLJ; Arritt et al. 1997; Cook et al. 2008; Feng et al. 2016; Gimeno et al. 2016; Nayak and Villarini 2017). The Great Plains LLJ has a diurnal cycle caused by thermal

gradient reversals over sloping terrain and frictional decoupling amid a rising boundary layer (Blackadar 1957; Fast and McCorcle 1990; Holton 1967; Jiang et al. 2007; Mitchell et al. 1995; Parish et al. 1988; Parish and Oolman 2010; Shapiro et al. 2016). The Great Plains LLJ peaks at nighttime at a height just above the boundary layer, between 925 and 850 hPa (Banta et al. 2002; Whiteman et al. 1997). It effectively transports heat and moisture from the Gulf of Mexico, providing an ideal thermodynamic environment for convection and precipitation at its jet exit (Higgins et al. 1997; Hodges and Pu 2019; Pu and Dickinson 2014; Weaver et al. 2009a). Low-level moisture fluxes are known to peak in July, with values sometimes greater than $200 \text{ kg m}^{-1} \text{ s}^{-1}$ (Weaver and Nigam 2008).

Previous studies have uncovered Great Plains LLJ large-scale, low-frequency variability that contributes to its interannual and intraseasonal fluctuations. Weaver and Nigam (2008) connected a strengthened Great Plains LLJ to positive anomalous diabatic heating in the eastern tropical Pacific. They also related the Great Plains LLJ to the negative phase of the 700-hPa geopotential height North Atlantic Oscillation (NAO), with a temporal correlation of -0.46 . They also showed that the difference

 Denotes content that is immediately available upon publication as open access.

Corresponding author: Kelsey Malloy, kelsey.malloy@rsmas.miami.edu

DOI: 10.1175/WAF-D-19-0103.1

© 2020 American Meteorological Society. For information regarding reuse of this content and general copyright information, consult the [AMS Copyright Policy](https://www.ametsoc.org/PUBSReuseLicenses) (www.ametsoc.org/PUBSReuseLicenses).

between the first two empirical orthogonal function modes of Great Plains LLJ variability depended on its connection to its moisture source, the Gulf of Mexico.

Multiple studies suggested that a negative Pacific–North America (PNA) teleconnection has a strong influence on the Great Plains LLJ on pentad and/or monthly time scales (Harding and Snyder 2015; Mallakpour and Villarini 2016; Nayak and Villarini 2017; Patricola et al. 2015). Harding and Snyder (2015) found that 78% of extreme rainfall events in the north-central United States exhibited a negative PNA signal within two weeks prior. It is suggested that tropically forced teleconnections, such as the PNA, have an important role in North American LLJ variability (Ting and Wang 1997; Trenberth and Guillemot 1996; Weaver et al. 2016), though there is debate on whether the 500-hPa pattern is truly forced by tropical Pacific activity in the midsummer months (Ding et al. 2011; Zhu and Li 2016). From a practical standpoint, the PNA teleconnection pattern has potential for submonthly forecasting based on its variability on medium-range time scales (Barnston and Livezey 1987; Feldstein 2000).

Currently, monthly predictions of mid to late-summer circulation are heavily influenced by SST anomaly conditions. Opposite SST anomalies in the tropical Pacific and North Atlantic often result in low-level circulation patterns that favor Great Plains LLJ strengthening (Hu and Feng 2012; Patricola et al. 2015; Weaver et al. 2009b; Weaver 2013; Weaver et al. 2016; Yu et al. 2017). Spring LLJs have been linked to the cool phase of El Niño–Southern Oscillation (ENSO), whereas the summer LLJ has been linked to the warm phase (Danco and Martin 2018; Krishnamurthy et al. 2015; Ting and Wang 1997; Trenberth and Guillemot 1996; Yu et al. 2016). ENSO state influences a circulation response, but the moisture supply for the extreme events originates in the subtropical Atlantic (Li et al. 2016; Li et al. 2017; Veres and Hu 2013). Therefore, both basins play a role in driving precipitation events, though their responses have intra-seasonal variations.

The Caribbean LLJ has a positive correlation with the Great Plains LLJ moisture transport (Mestas-Núñez et al. 2007; Wang 2007; Krishnamurthy et al. 2015). ENSO's modulation on the Caribbean LLJ is different from spring to summer as well. In summer, easterlies are enhanced by an El Niño state. In conjunction with a cool Atlantic state, or negative Atlantic multidecadal oscillation (AMO) phase, the oppositely phased SST anomalies and strong Caribbean LLJ are associated with stronger southerlies into the Great Plains region. The temporal correlation between the Caribbean LLJ and Great Plains LLJ is 0.47 for the summer months

(Krishnamurthy et al. 2015). Dirmeyer and Kinter (2010) also commented on the Caribbean Sea being a significant moisture source for extreme precipitation events, such as summer of 1993. Caribbean LLJ strength is an indicator of the modulation of the North Atlantic subtropical high and its associated moisture transport capabilities into the Great Plains (Wang 2007).

Anomalous soil moisture may fuel summertime precipitation events, but the response time is inconclusive. Li et al. (2016) and Li et al. (2017) demonstrated that the Great Plains LLJ responds to wet soil dynamically and thermodynamically, causing it to strengthen in general. Weaver et al. (2009a) suggested that soil moisture had a relatively small effect on the evolution of hydroclimate extremes, and here we focus on the large-scale dynamical influences of extremes. In addition, the North American Rocky Mountains is an important feature when simulating Great Plains LLJ activity as it strongly participates in stationary wave modulation (Byerle and Paegle 2003; Ting and Wang 2006; Weaver and Nigam 2011), but topographical considerations are beyond the scope of this paper.

The primary objective in this study is to analyze large-scale, low-frequency variability features in a predictive framework by employing an ensemble approach. Here we use the Community Climate System Model, version 4 (CCSM4), forecasts to assess the skill in predicting anomalous Great Plains LLJ events. There are three main research questions addressed here:

- 1) Are the CCSM4 forecasts able to reproduce the interannual variability of the Great Plains LLJ and its associated extreme midsummer Plains and Midwest precipitation?
- 2) Are there relatively consistent large-scale sources of predictability for midsummer forecasts out to a month?
- 3) Are these large-scale predictors from point 2 above able to provide a “forecast of opportunity” (i.e., confidence in forecast increases when large-scale predictor exhibits its expected signal for an event)?

In the following study, there is evidence that suggests that each analyzed source of predictability has a robust relationship with the Great Plains LLJ. However, the circulation predictors, rather than SSTs, provide the forecast of opportunity. SST forecast skill is already relatively high and the ensemble members are typically in agreement with these relatively short lead times. Circulation predictors have relatively lower skill and their potential relies on ensemble agreement (forecast confidence). Section 2 presents the data and methods used to produce and analyze the results. Section 3 describes the results, organized into subsections about the

model's skill, potential sources of predictability and its forecast value, and case study investigation. Last, [section 4](#) provides a summary and more detailed discussion of these results.

2. Data and methods

a. Model and observations

The forecast model used for this study is the National Center Atmospheric Research (NCAR) CCSM4. It is currently being used for routine real-time predictions (<http://www.cpc.ncep.noaa.gov/products/NMME/>) as part of North American Multi-Model Ensemble (NMME; [Kirtman et al. 2014](#)). The analysis presented here focuses on CCSM4 retrospective forecasts primarily because the data needed to assess LLJs are readily available to the research team, whereas the data from the other NMME models in the public archive do not include sufficient vertical resolution to capture the LLJs. Moreover, the data in the multimodel archive only include data up through 2010, where we consider data up through 2016. Finally, we also make comparisons with extended control simulations, which are also not readily available for all the NMME models. In this study, the 10 ensemble members of CCSM4 have a spatial resolution of 1° latitude \times 1° longitude. They are initialized every 1 July between 1982 and 2016 and analyzed as the July monthly average unless noted otherwise. July was chosen because mechanisms for modulating the Great Plains LLJ often differ when comparing spring (April–June) and late summer/early fall (August–October). July possesses characteristics from both subseasons, has the highest correlation with regional precipitation, and is most representative of summertime circulation patterns ([Weaver and Nigam 2008](#); [Weaver et al. 2009a,b](#)). CCSM4 is a fully coupled atmosphere–ocean model in which the atmosphere, ocean, and land are initialized from Climate Forecast System Reanalysis (CFSR), and ensemble generation is determined by the time-lagged method (i.e., ensembles take initial conditions from different yet consecutive output times of CFSR around 1 July). A discussion of the initialization procedures are described in some detail in [Kirtman and Min \(2009\)](#), [Paolino et al. \(2012\)](#) and [Infanti and Kirtman \(2016\)](#). The results regarding climatology include analysis from the free-running CCSM4, which is not initialized as the forecast version (“cold start”).

The Modern-Era Retrospective Analysis for Research and Applications, version 2 (MERRA-2) is a global retrospective reanalysis dataset that provides subdaily estimates beginning in 1980 ([Bosilovich et al. 2015](#); [Gelaro et al. 2017](#)). For temporal consistency with

the CCSM4 forecasts, analysis begins in 1982 and extends through 2016. MERRA-2's spatial resolution is 0.5° latitude \times 0.625° longitude but is bilinearly interpolated on the CCSM4 grid when necessary for comparison. Most of the monthly and daily meteorological variables in this study are from MERRA-2 data. Precipitation values are taken from the Climate Prediction Center (CPC) unified gauge-based analysis, which provides daily data over conterminous United States with a $0.25^\circ \times 0.25^\circ$ spatial resolution ([Chen et al. 2008](#); [Xie et al. 2007](#)).

The Extended Reconstructed Sea Surface Temperature, version 5 (ERSST-5) provides monthly, global SST data from the International Comprehensive Ocean–Atmosphere Dataset (ICOADS; provided by the NOAA/OAR/ESRL PSD, Boulder, Colorado, USA, from their website at <https://www.esrl.noaa.gov/psd/>). It incorporates in situ data on a $2^\circ \times 2^\circ$ grid and represents spatial variability of SSTs well ([Huang et al. 2017](#)). Anomalies are set as deviations from the 1971–2000 average.

b. Indices

The LLJ index is defined as the averaged 900-hPa meridional wind (V900) in the domain 25° – 35° N, 102° – 97° W, and the Great Plains precipitation index is defined as the averaged precipitation in the domain 35° – 45° N, 100° – 90° W ([Weaver and Nigam 2008](#)). The Caribbean LLJ index is the averaged 900-hPa zonal wind (U900) in the domain 12.5° – 17.5° N, 80° – 70° W ([Wang 2007](#)). The index is multiplied by -1 to make the easterlies positive, a more straightforward way to relate the relationship between a strengthened Caribbean LLJ and Great Plains LLJ. These domains are outlined in relevant figures.

CPC (<http://www.cpc.ncep.noaa.gov/>) has a methodology for calculating the PNA, AMO, and Niño-3.4 indices. This study uses similar methodologies, including standardizing all indices over the time series. The PNA is defined as $[Z^*(15^\circ$ – 25° N, 180° – 140° W) $-$ $Z^*(40^\circ$ – 50° N, 180° – 140° W) $+$ $Z^*(45^\circ$ – 60° N, 125° – 105° W) $-$ $Z^*(25^\circ$ – 35° N, 90° – 70° W)], where Z^* denotes monthly mean 500-hPa height (Z500) anomaly that is obtained by subtracting the July mean value between 1982 and 2016. Niño-3.4 is defined as $[T^*(5^\circ$ S– 5° N, 170° – 120° W)], where T^* denotes SST anomalies from ERSST-5 or CCSM4. The AMO index is defined as ocean-only $[T^*(0^\circ$ – 70° N, 80° W– 0°)], where T^* denotes SST anomalies from ERSST-5 or CCSM4.

c. Skill scores

There is an assortment of skill metrics used to compare MERRA-2 to CCSM4 forecasts. The anomaly correlation

coefficient is a well-known statistic that essentially analyzes the agreement of the anomaly's sign between the observation and model ensemble mean (Wilks 1995). Here it is done on a gridpoint-by-gridpoint basis. A negative value indicates opposing anomalies and a higher, positive value indicates higher agreement between forecast and observed anomalies.

The ranked probability skill score (RPSS) relates the forecast skill to a reference forecast—in this case, climatology—by considering how far the forecast's cumulative distribution function is from the observed outcome (Weigel et al. 2007). This is better for categorical probability forecasts. In this case, V900 and precipitation are separated into strong, moderate, and weak events using tercile distribution. RPSS is also done on a gridpoint-by-gridpoint basis.

The anomaly correlation coefficient and RPSS are also used to measure homogeneous predictability. Homogeneous predictability demonstrates the model's ability to predict itself (Becker et al. 2014). One ensemble member is treated as “truth” (in this study, ensemble 10 was chosen arbitrarily), and the skill scores are reassessed in a perfect model assumption. This is a way to gauge how the model perceives its predictability of the LLJ and precipitation; a relatively high score suggests physical mechanisms may exist that influence ensemble agreement.

Finally, root-mean-square (RMS) error and RMS spread is used for discussing the model's progression throughout the month (Simmons et al. 1995). RMS error compares the ensemble mean to observation, and RMS spread averages the distance between each ensemble and the ensemble mean. In an ensemble framework, the ratio of spread to error should be 1:1 throughout the month because ensemble disagreement should be proportional to potential error as the lead time increases. A small ratio would indicate an overconfident ensemble set since the spread is not correctly signaling lack of agreement between ensemble mean and observation.

d. Predictor analysis

By comparing the large-scale teleconnection patterns of CCSM4 forecasts and MERRA-2, a consistent link between the standardized index and V900 in the model provides an opportunity for forecasters. Linear regressions determine “slope” associations between variables and the index time series. It may also help explain discrepancies in atmospheric response between the model and reanalysis. The results reflect the mean from each ensemble member's regression rather than a regression from the ensemble mean. In this study, the percentages of ensembles that agree with the sign in the Great Plains LLJ region are superimposed, an advantage of this

approach. It is only considered valuable if at least 70% of the ensembles agree in the LLJ index region.

Kernel density estimators (KDEs) are smoothed histograms that can be analyzed like nonparametric probability density functions. One can identify whether the distribution shifts of a sample set are statistically different from the group containing all values using KDEs. Here, each large-scale predictor identified by the linear regression is used as a criterion for creating a sample set of V900 in the LLJ index region to be compared with the group consisting of total V900 values in LLJ index region for all months. In addition, pairs of these sources are grouped; a sample set is created when two predictors are occurring simultaneously. The selected pairs in results (circulation predictors, Pacific predictors, Atlantic predictors) are examples of potential background states aimed to isolate the circulation influences and the influences from each ocean basin. Note that all KDE shifts in the results will be statistically significant (p value < 0.05).

e. Case study setup

Four case studies were chosen in order to better understand the CCSM4 forecasts' strengths and weaknesses in addition to demonstrating the realistic uses of these sources of predictability. The case studies were chosen based their positive or negative precipitation anomaly from the observational Great Plains precipitation index, such that two cases would be considered well-known wet events and two cases would be considered well-known dry events. Then, these categories were further split to include one well-forecasted event and one poorly forecasted event. The chosen cases are taken from every decade of the study's range of years. The four cases are as follows:

- 1) 1988—Good forecast, dry anomaly
- 2) 1993—Good forecast, wet anomaly
- 3) 2003—Bad forecast, dry anomaly
- 4) 2016—Bad forecast, wet anomaly

Cases are used to compare large-scale circulation and climate variability patterns to better locate any potential forecasting opportunities when using the CCSM4 or similar model. The objective of this analysis is to provide insight into impactful events, decomposing the key differences between predictors of good and bad forecasts to determine which predictors are more advantageous when assigning forecast confidence. Last, the spatial signal-to-noise ratio will assess the applicability of using monthly mean values for the circulation predictors. The signal-to-noise ratio takes the variance of monthly data and divides by the average variance of the daily data from the monthly mean. Climate forecasting relies on persistence of background flow; therefore, locations

July Climatology for V900

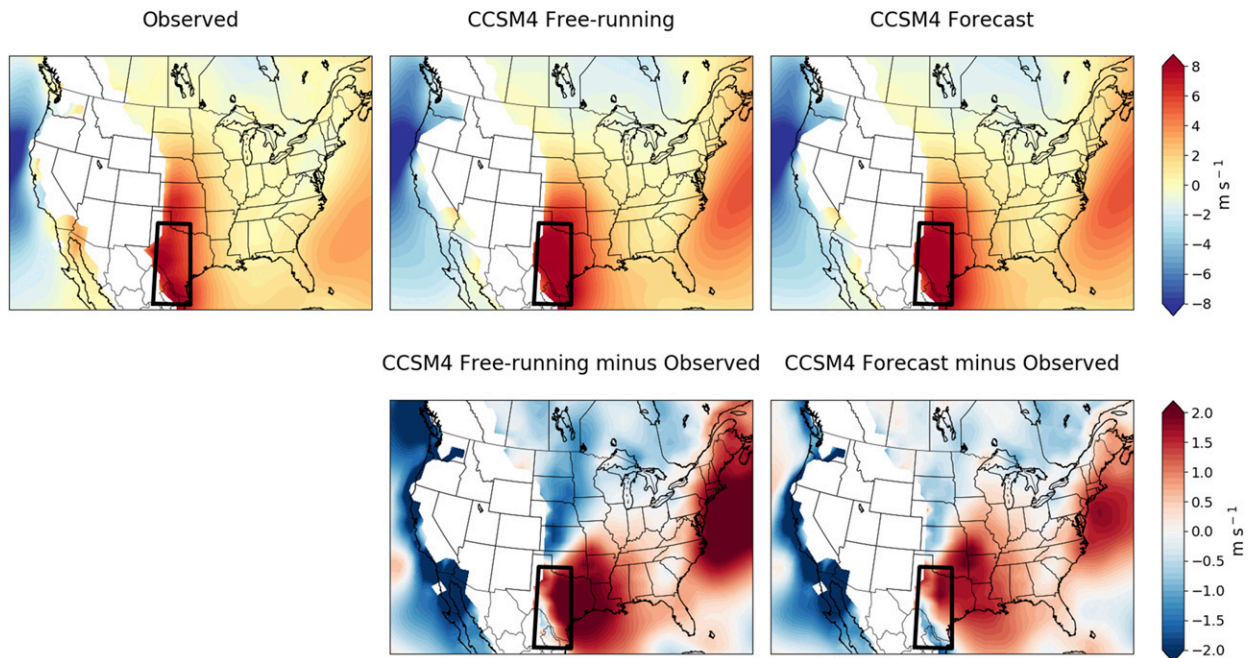


FIG. 1. July climatology for V900 for (top left) MERRA-2, (top center) CCSM4 free running model, and (top right) CCSM4 forecast model. (Bottom center) Subtraction difference between CCSM4 free running model and MERRA-2 climatology. (Bottom right) Subtraction difference between CCSM4 forecast model and MERRA-2 climatology. Boxes indicate LLJ index domain.

with relatively high signal-to-noise ratios of Z500 and U900 are more beneficial when forecasting past two weeks when the signal is sufficiently large compared to the noise.

3. Results

a. CCSM4 skill evaluation

Model skill is first evaluated by calculating climatological bias between the CCSM4 and the reanalysis or observational data. CCSM4 produces a July climatological Great Plains LLJ that resembles the one in MERRA-2, though the difference between the two reveals immediate biases. The model Great Plains LLJ is too strong—greater by 2 m s^{-1} —and extends too far east (Fig. 1, bottom row). However, the forecast model shows slight improvement over the free-running model, supporting that initialization does improve the prediction of climatology. The climatological vertical profile of the meridional wind in the LLJ index region for both MERRA-2 and CCSM4 forecasts, seen in Fig. 2, reveals that the meridional wind is overestimated in the entire layer below 850 hPa in CCSM4 and the peak occurs at 925 hPa instead. This does raise concerns about using 900 hPa as the level for evaluating the Great Plains LLJ. However, because the entire layer is consistently

overestimated, and the reanalysis shows the peak at 900 hPa, it remains an appropriate choice. CCSM4 forecast precipitation climatology (Fig. 3) exposes the several challenges in precipitation prediction, but most important to this study is that the Plains/Midwest is $1\text{--}2 \text{ mm day}^{-1}$ too dry. It is also noted that the Southeast United States is $1\text{--}2 \text{ mm day}^{-1}$ too wet. The Southeast U.S. precipitation may be dynamically related to Great Plains LLJ events through background circulation (Pu et al. 2016). However, while some results pertain to Southeast U.S. precipitation forecasting, it will not be a focus due to its limited connection to the Great Plains LLJ.

The anomaly correlation coefficient and RPSS for the CCSM4 forecasts reveal strengths and weaknesses in representing variability (Fig. 4). Anomaly correlation coefficient for V900 shows relatively large skill in the jet core (0.5–0.6), and the anomaly correlation coefficient for precipitation is relatively high in the jet entrance and exit (0.4–0.5). RPSS is largely consistent with anomaly correlation coefficient but also highlights problematic areas. Once more, the best RPSS score for V900 remains in the climatological jet (0.3–0.4) and sharply decreases east of the jet (<0), where the negative RPSS indicates a forecast worse than assuming climatology. There is modest precipitation skill at the jet entrance and jet exit (0.1–0.2), but the skill over the rest of the

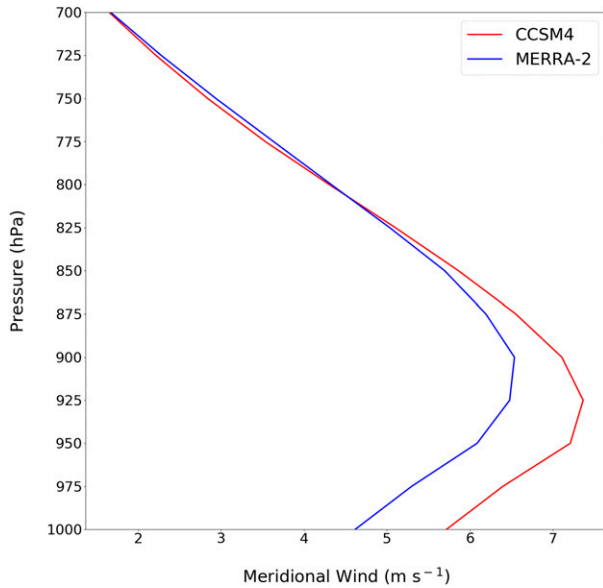


FIG. 2. Average meridional wind as a function of pressure level in LLJ index region (outlined in Fig. 1); the red line shows CCSM4 climatology and the blue line shows MERRA-2 climatology.

Great Plains and Midwest region is low or worse than assuming climatology.

The homogeneous predictability skill scores improve almost everywhere, as expected, reaching a maximum anomaly correlation coefficient in the jet core (0.6–0.7)

and at the precipitation entrance and exit (0.4–0.5), seen in Fig. 5. The CCSM4 suggests a physical, predictable climate feature. In addition, the hot spots of relatively high scores are different, which illustrates the differences in variability between observation and the CCSM4 forecasts. For example, relatively high homogeneous predictability scores around the bottom-right corner of the Great Plain Precipitation index domain suggest a mechanism in the model that places a predictable precipitation signal there. This hot spot is farther east from what real forecast skill indicates. This is consistent with above results revealing that the model simulates a climatological Great Plains LLJ that extends too far to the east.

July daily data reveal how much skill is related to initialization. During the first two weeks, the highest anomaly correlation coefficient scores are located in the jet core (0.2; Fig. 6). The anomaly correlation coefficient plummets further during the last couple weeks of the month. In addition, the ratio of RMS spread to RMS error ranges from 0.5 to 0.8 in first two weeks and sharply increases to 0.8–1 in last two weeks. The attribution of any skill within the first two weeks is most likely due to initialization, and the lower ratio of RMS spread to error signals overconfidence. Erroneous jet events may result from poor simulations of changing circulation responses after the first week or two as the CCSM4 ensembles diverge.

July Climatology for Precipitation

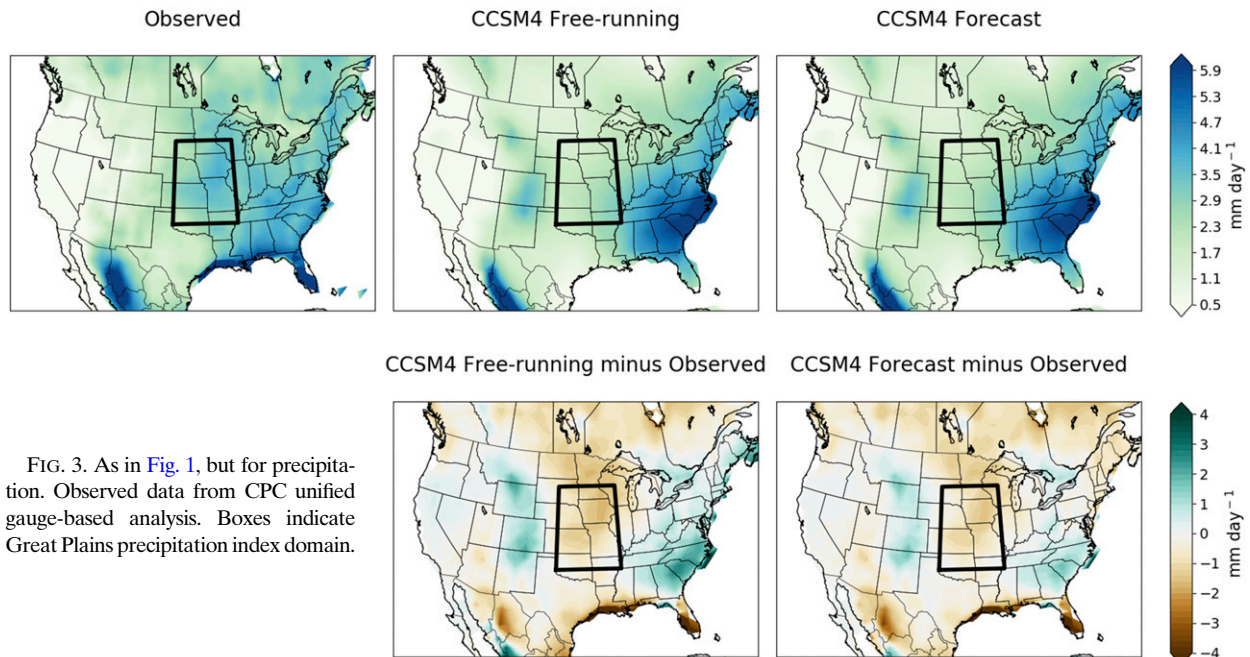


FIG. 3. As in Fig. 1, but for precipitation. Observed data from CPC unified gauge-based analysis. Boxes indicate Great Plains precipitation index domain.

Skill Scores

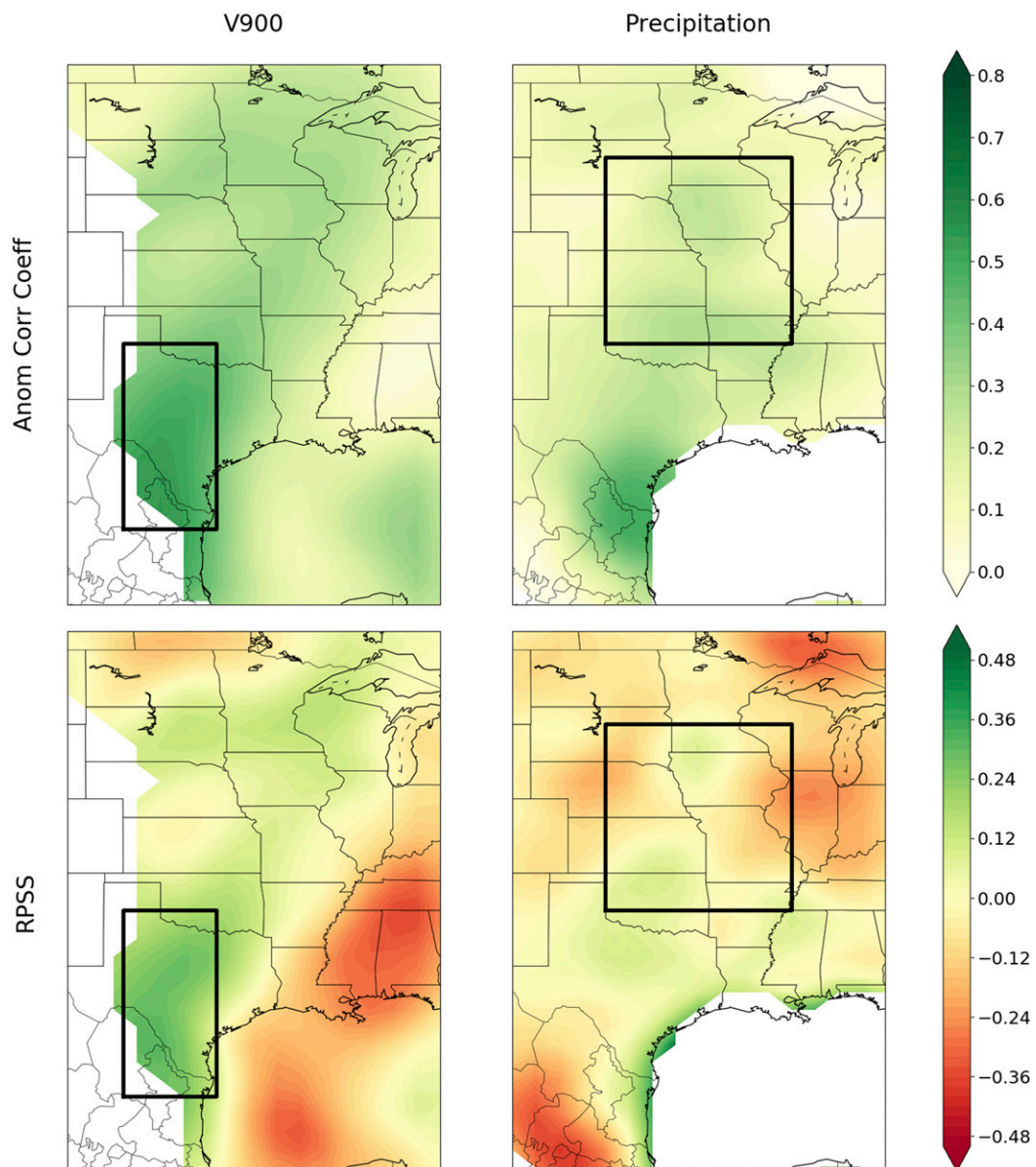


FIG. 4. Anomaly correlation coefficient scores for (top left) V900 and (top right) precipitation. RPSS for (bottom left) V900 and (bottom right) precipitation. Data have been spatially smoothed using a Gaussian filter.

The skill scores and ratio between RMS spread and RMS error further motivates the need for additional large-scale predictors of precipitation. Background flow at initialization is a key factor in building confidence in forecasts of Great Plains LLJ and, hence, rainfall events. The Caribbean LLJ, PNA, ENSO, and AMO are the chosen large-scale teleconnections in this study due to their connection to the Great Plains LLJ in previous literature and their quasi-persistent nature. Therefore,

the following analysis will focus on quantitatively relating this set of large-scale teleconnections to the Great Plains LLJ as well as comparing the jet responses between MERRA-2 and CCSM4.

b. Identifying predictors

Weaver and Nigam (2008) found that the temporal correlation between the Great Plains LLJ and precipitation indices in July is 0.71. CCSM4 does produce wet

Homogeneous Predictability

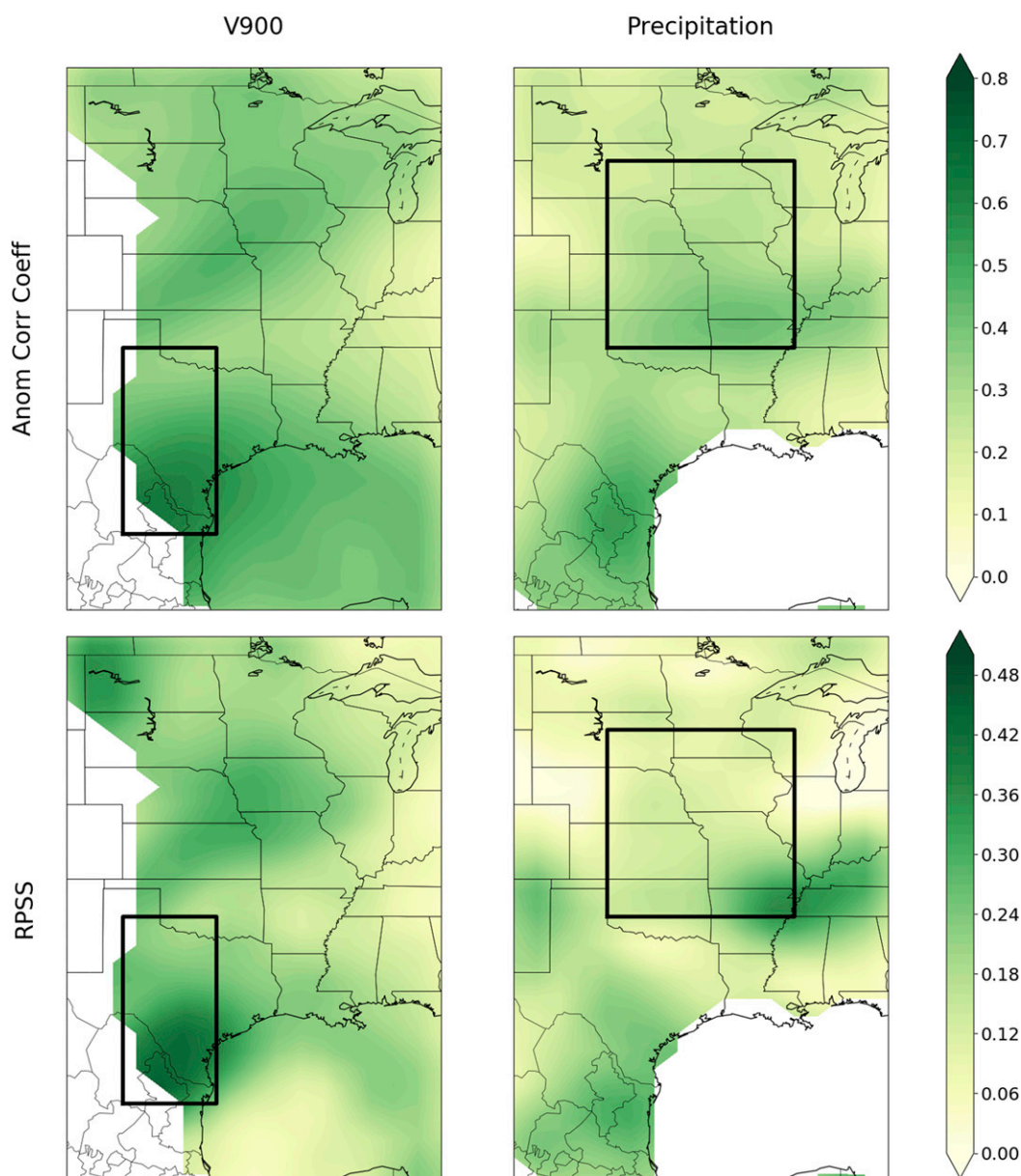


FIG. 5. Homogeneous predictability of CCSM4 forecasts. Ensemble 10 is used as “truth” for anomaly correlation coefficient scores and RPSS. Format is similar to Fig. 4.

conditions in the Great Plains and Midwest during Great Plains LLJ events, but this relationship is underestimated (Fig. 7). Since the index is standardized, it can be interpreted that for $+1\sigma$ LLJ events, observations indicate a $1\text{--}2\text{ mm day}^{-1}$ increase in rainfall over the Midwest and northern Plains. In CCSM4, this response peaks at 0.5 mm day^{-1} and extends eastward into the Great Lakes region. V900 and the LLJ index are established as potential predictors

or proxies for Great Plains precipitation activity, though there are difficulties in representing the variability.

CCSM4 captures a positive relationship between the Caribbean LLJ and Great Plains LLJ (Fig. 8). This signals that there is an extension of the above-normal easterlies from the North Atlantic subtropical high into the Caribbean that is related to the strengthening of the Great Plains LLJ. The Caribbean LLJ is the chosen

CCSM4 V900 Skill Limit

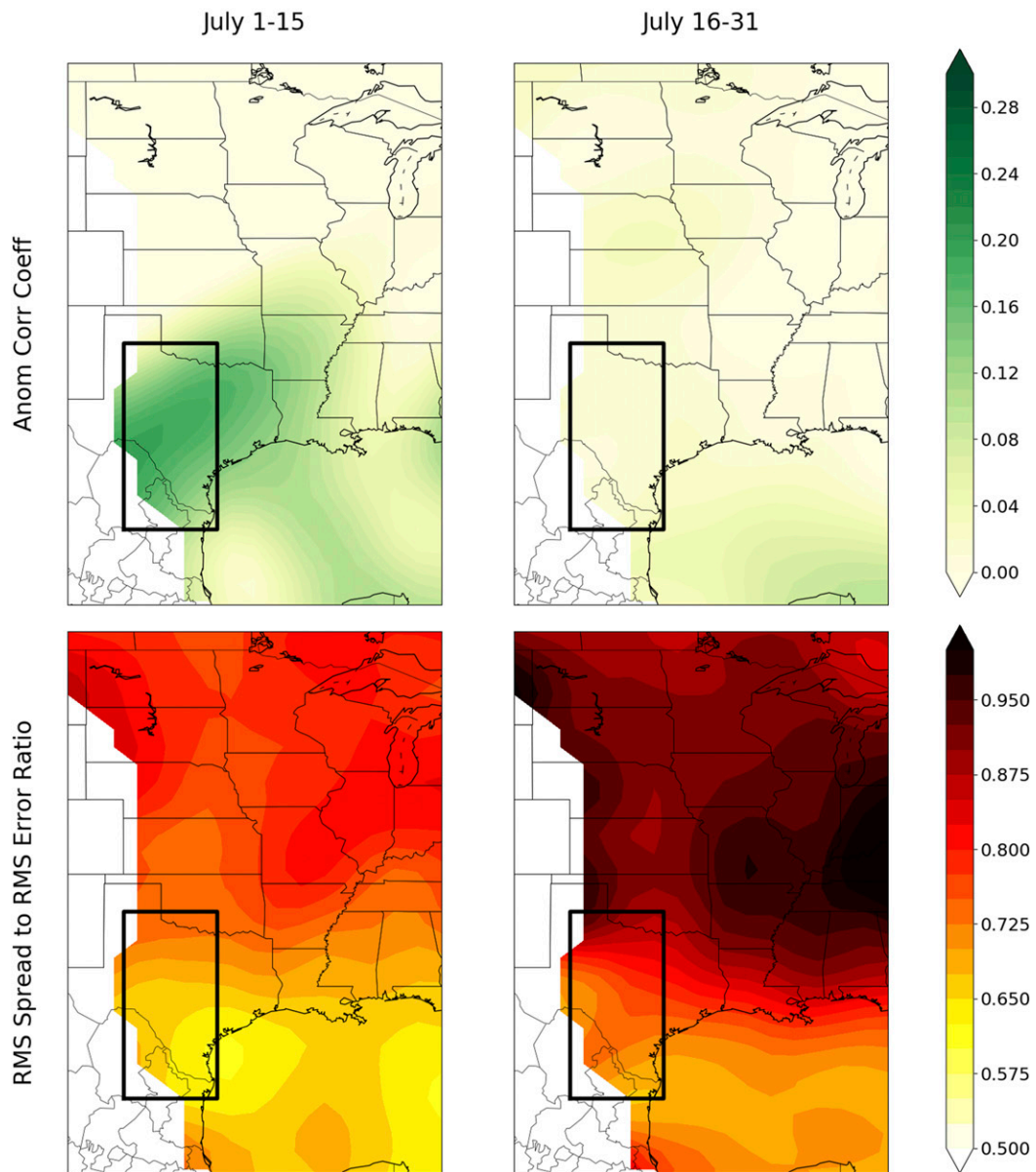


FIG. 6. Anomaly correlation coefficient scores for CCSM4 for (top left) 1–15 Jul and (top right) 16–31 Jul. Ratios of RMS spread to RMS error for (bottom left) 1–15 Jul and (bottom right) 16–31 Jul. Data has been spatially smoothed using a Gaussian filter.

indicator for North Atlantic subtropical high modulation rather than the NAO in this framework. The NAO regression onto V900 did not reach the 70% ensemble agreement threshold in the LLJ region. As mentioned in the introduction, the Caribbean LLJ also includes moisture supply information from the Caribbean Sea. Fortunately, the circulation response outside the jet region in CCSM4 is comparable in magnitude to MERRA-2 ($+0.8 \text{ m s}^{-1}$).

A negative PNA phase is linked to a strengthened Great Plains LLJ (Fig. 9). The 900-hPa total moisture transport (VQ900) is shown instead of V900 to demonstrate the importance of the jet’s attachment to the Gulf of Mexico as a moisture support. CCSM4’s depiction is shifted northward—away from the moisture source—compared to MERRA-2, which could reduce or alter precipitation processes. Furthermore, the regressions are relatively comparable, though the

Regression of LLJ Index onto Precipitation

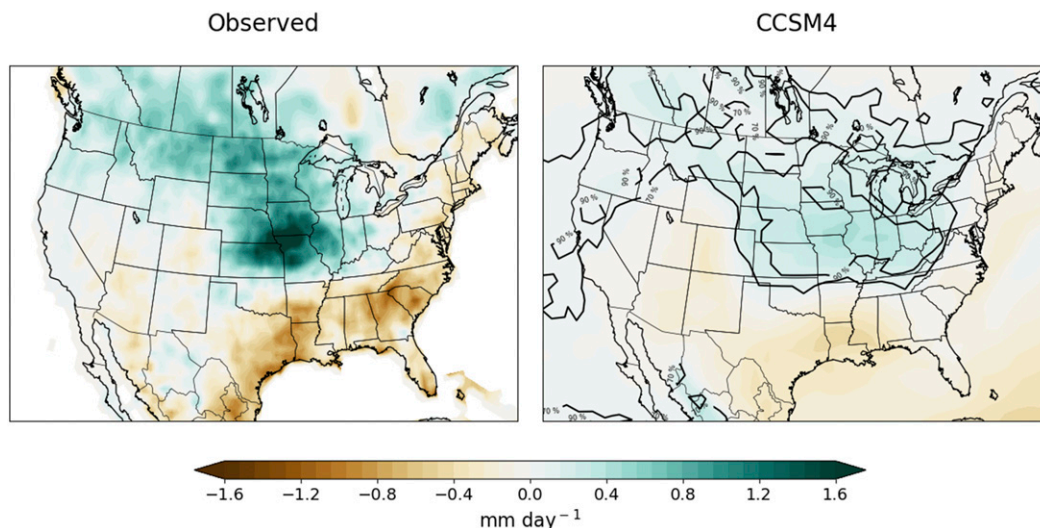


FIG. 7. Regression coefficient for $+1\sigma$ LLJ events onto precipitation for (left) MERRA-2 (LLJ index) and CPC unified gauge-based analysis (precipitation data), and (right) CCSM4. The solid black contours for CCSM4 indicate 70% and 90% ensemble agreement about a positive anomaly.

magnitude of CCSM4's regression is only half of MERRA-2's regression (-8 and $-15 \text{ m s}^{-1} \text{ g kg}^{-1}$, respectively). The circulation response outside the jet region is also comparable, similar to the Caribbean LLJ regression, supporting the idea that the monthly PNA and Caribbean LLJ present a forecast of opportunity (i.e., an expected signal bolsters forecast confidence in Great Plains LLJ predictions). Large-scale circulation changes, such as the Caribbean LLJ

and PNA, often reflect an atmospheric response to SST anomalies. Therefore, SST variability may be an important influence on circulation changes, and knowing the phase of the tropical Pacific and northern Atlantic SST is a component in understanding Great Plains LLJ modulation.

ENSO and AMO have separate effects on the Great Plains LLJ, but it would be beneficial to understand their possible constructive and destructive interference.

Regression of CLLJ Index onto V900

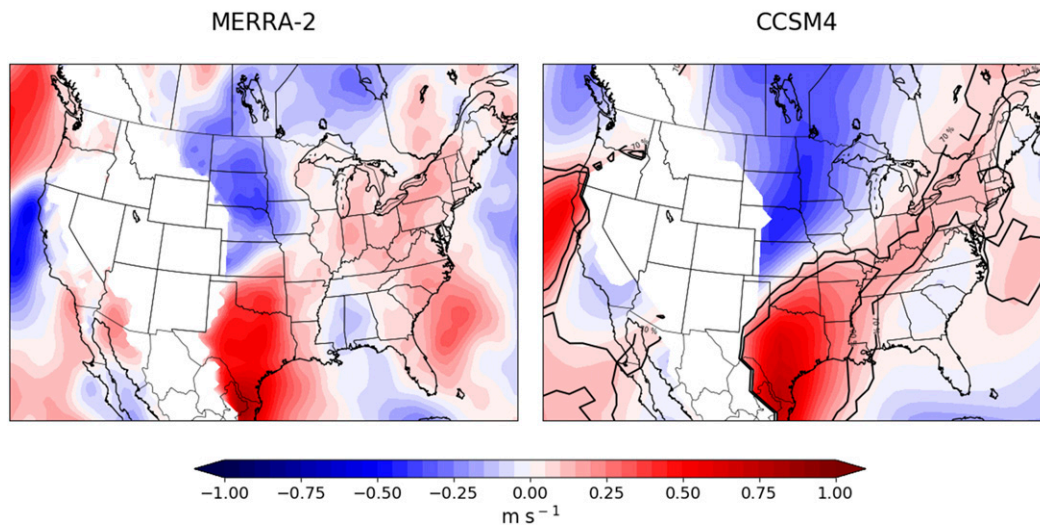


FIG. 8. Regression coefficient for $+1\sigma$ Caribbean LLJ events onto V900 for (left) MERRA-2 and (right) CCSM4. The solid black contours for CCSM4 indicate 70% and 90% ensemble agreement about a positive anomaly.

Regression of PNA Index onto 900 hPa Total Meridional Moisture Transport

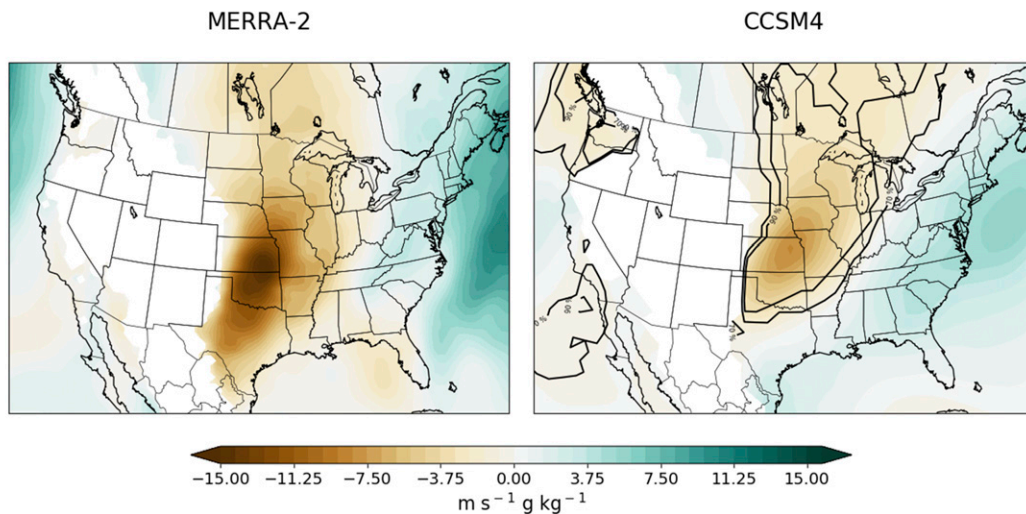


FIG. 9. Regression coefficient for $+1\sigma$ PNA events onto 900-hPa total meridional moisture transport for (left) MERRA-2 and (right) CCSM4. The solid black contours for CCSM4 indicate 70% and 90% ensemble agreement about a negative anomaly.

A warm phase of Niño-3.4 and a cool phase of AMO are associated with a strengthened Great Plains LLJ (Fig. 10). Weaver et al. (2009b) and Hu and Feng (2012) suggest that Pacific and Atlantic SSTs have a quasi-linear relationship regarding their circulation responses. Therefore, by adding the responses, there is some indication of whether there is constructive or destructive interference (i.e., if the effect of ENSO and AMO amplifies the Great Plains LLJ response anomaly or reduces it). In MERRA-2, the regression from multidecadal variability of the Atlantic (-1.2 m s^{-1}) overwhelms the regression from interannual variability of the tropical Pacific ($+0.8 \text{ m s}^{-1}$), and not just for the Great Plains LLJ but the entire eastern United States. Arguably, their combined effects are small and may even “wash out” any Great Plains LLJ signal. By contrast, CCSM4 shows approximately half the regression slope of both AMO and ENSO (-0.6 and $+0.4 \text{ m s}^{-1}$, respectively), and their cumulative effects result in a central-eastern U.S. dipole of meridional wind, favoring the AMO phase when linearly associating SST anomalies to a Great Plains LLJ response. In general, there are large differences between MERRA-2 and CCSM4 in terms of how the eastern United States responds to SST variability. One may argue that the proper sign in the Great Plains LLJ region suggests that ENSO and AMO may still be advantageous predictors of the jet, but future analysis is needed to better understand the overall circulation response to ENSO and AMO separately in CCSM4.

These predictors are summarized in the following KDEs by comparing the total group of V900 values

in the LLJ region with a subset of V900 values during common example background states. As mentioned before, all the KDE shifts from MERRA-2 and CCSM4 have a p value < 0.05 , which shows that the relationships from Figs. 8–10 are significant in the LLJ region. The MERRA-2 KDEs reveal that individual predictors shift the distribution about $+0.5 \text{ m s}^{-1}$, but this is not as large as if two predictors were present simultaneously (Fig. 11). The other panels indicate that circulation influences (positive Caribbean LLJ and negative PNA), Pacific influences (El Niño and negative PNA), and Atlantic influences (negative AMO and positive Caribbean LLJ) all show large shifts of the mean (about $+1.5$, $+0.9$, and $+1.2 \text{ m s}^{-1}$, respectively). The results for CCSM4 (Fig. 12) are similar. First, it is noted that the distributions for all groups are narrower, indicating an underestimation in the variability of V900 in this region. However, the KDE shift is the same direction as MERRA-2. Perhaps the largest forecast of opportunity results from the circulation influences and Atlantic influences (mean shift of $+0.6$ and $+0.5 \text{ m s}^{-1}$, respectively) since their KDE shift is comparable to MERRA-2.

c. Case study analysis

Figures 13 and 14 summarize the case studies of interest. The first two rows are well-known dry and wet years, 1998 and 1993, respectively, and the correct signs of V900 and precipitation in LLJ region are well-simulated in both the CCSM4 ensemble mean (middle column) and forecast probabilities (right column).

Regression of SST Indices onto V900

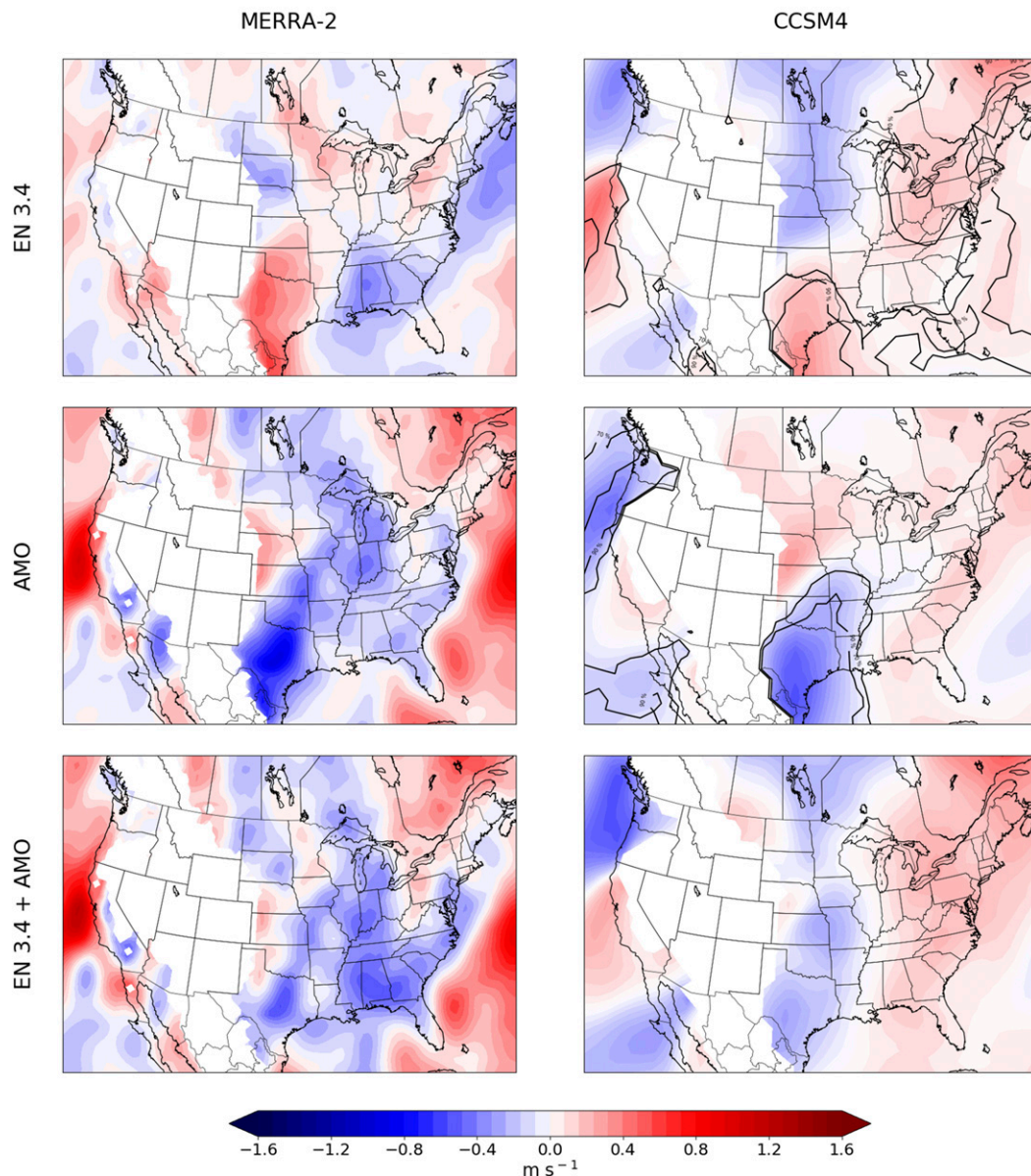


FIG. 10. Regression coefficient for $+1\sigma$ Niño-3.4 events onto V900 for (top left) MERRA-2 and (top right) CCSM4. (middle left),(middle right) As in the top row, but for $+1\sigma$ AMO events. (bottom left),(bottom right) Sum of regression coefficients from the top and middle rows. The solid black contours for CCSM4 in the top and middle rows indicate 70% and 90% ensemble agreement for expected anomaly in the Great Plains LLJ region.

Forecast probability plots arguably provide more information than ensemble means for depicting model output since they use all ensembles to consider a range of possible outcomes. 1993 has a $>90\%$ probability of an above-normal V900 event in the LLJ region, and 1988 has a $>50\%$ probability of a below-normal event (note that the climatological probability is 33%). As expected, the precipitation anomaly is located in the jet exit region

for the well-forecasted events. The bottom two rows are considered poorly simulated dry and wet events 2003 and 2016, respectively. While the CCSM4 ensemble mean has a negative V900 anomaly for 2003, it does not extend as far as with MERRA-2, and there is a positive V900 anomaly directly above that is not present in MERRA-2. The CCSM4 forecast shows a 90% probability of a jet event into the Southeast United States that

MERRA-2 KDEs of V900 in LLJ Index Region

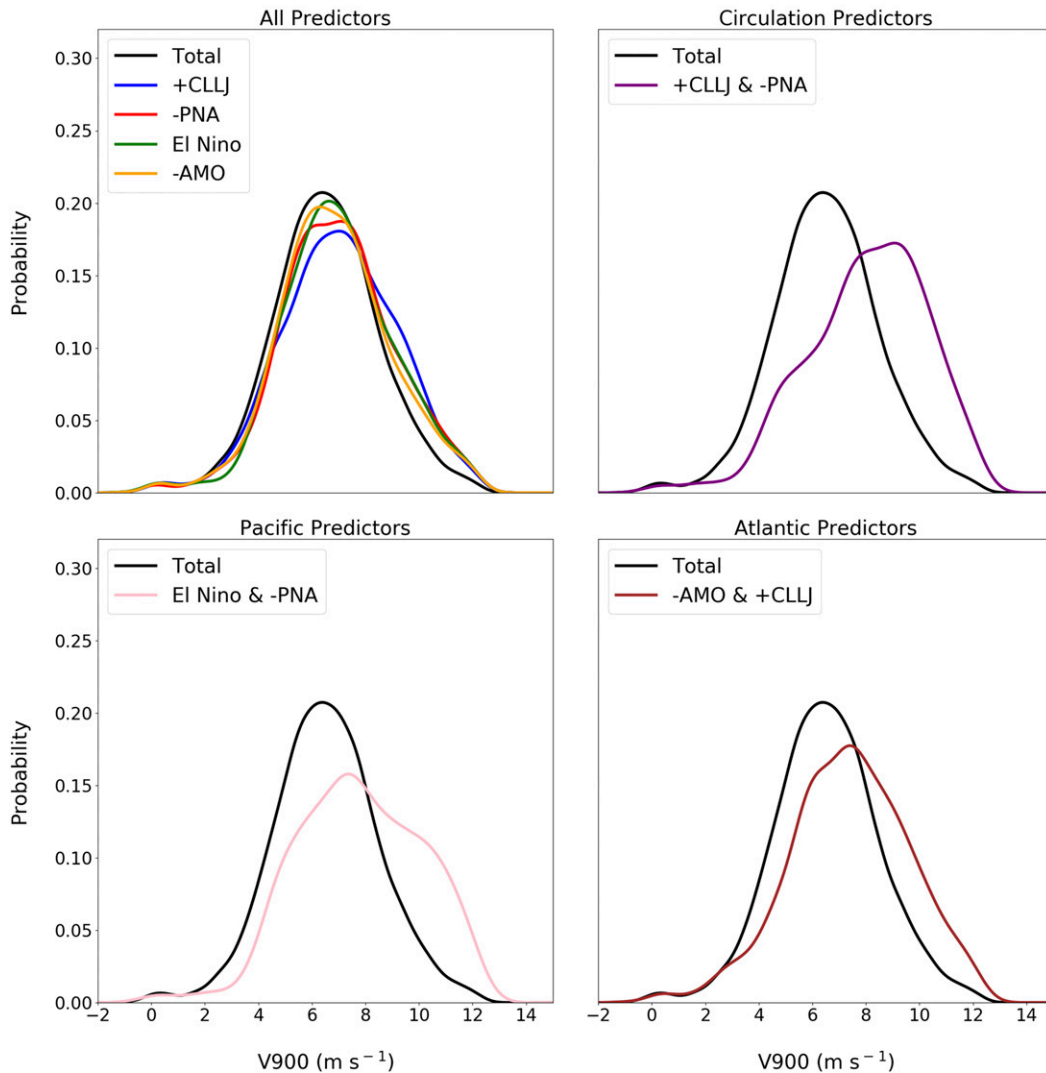


FIG. 11. MERRA-2 KDEs of V900 values in the LLJ index region for (top left) all predictors separately, (top right) circulation predictors occurring simultaneously, (bottom left) predictors in the Pacific Ocean basin occurring simultaneously, and (bottom right) predictors in the Atlantic Ocean basin occurring simultaneously. The black solid KDE in every panel contains the full set of V900 values.

is not detected in MERRA-2. This strong, eastward LLJ created an erroneous positive precipitation anomaly that is not present in MERRA-2; rather, MERRA-2 has a negative precipitation anomaly as a result of its prominent negative V900 anomalies. Last, the 2016 case in MERRA-2 shows a strong LLJ. CCSM4 does not capture the LLJ or the precipitation anomaly at all.

To understand the large-scale environment of these events and to try to apply the sources of predictability from the previous section's linear regressions, Fig. 15 decomposes the major differences between the SSTs and circulation in the good forecasts versus bad

forecasts. Note that forward (back) slashes correspond with dry 1988 and 2003 (wet 1993 and 2016) forecasts. Here we see that for both the Pacific and Atlantic, the SST anomalies are well-simulated in the CCSM4 forecasts, and the ensembles agree on the sign for both years. However, this is also the case for the bad forecasts, which is expected for one-month SST anomaly forecasts. CCSM4 correctly simulated the equatorial SST anomalies in the Pacific and the large-scale SST anomaly features in the North Atlantic basin. This example demonstrates that SST anomalies in both basins may not provide a forecast of opportunity

CCSM4 KDEs of V900 in LLJ Index Region

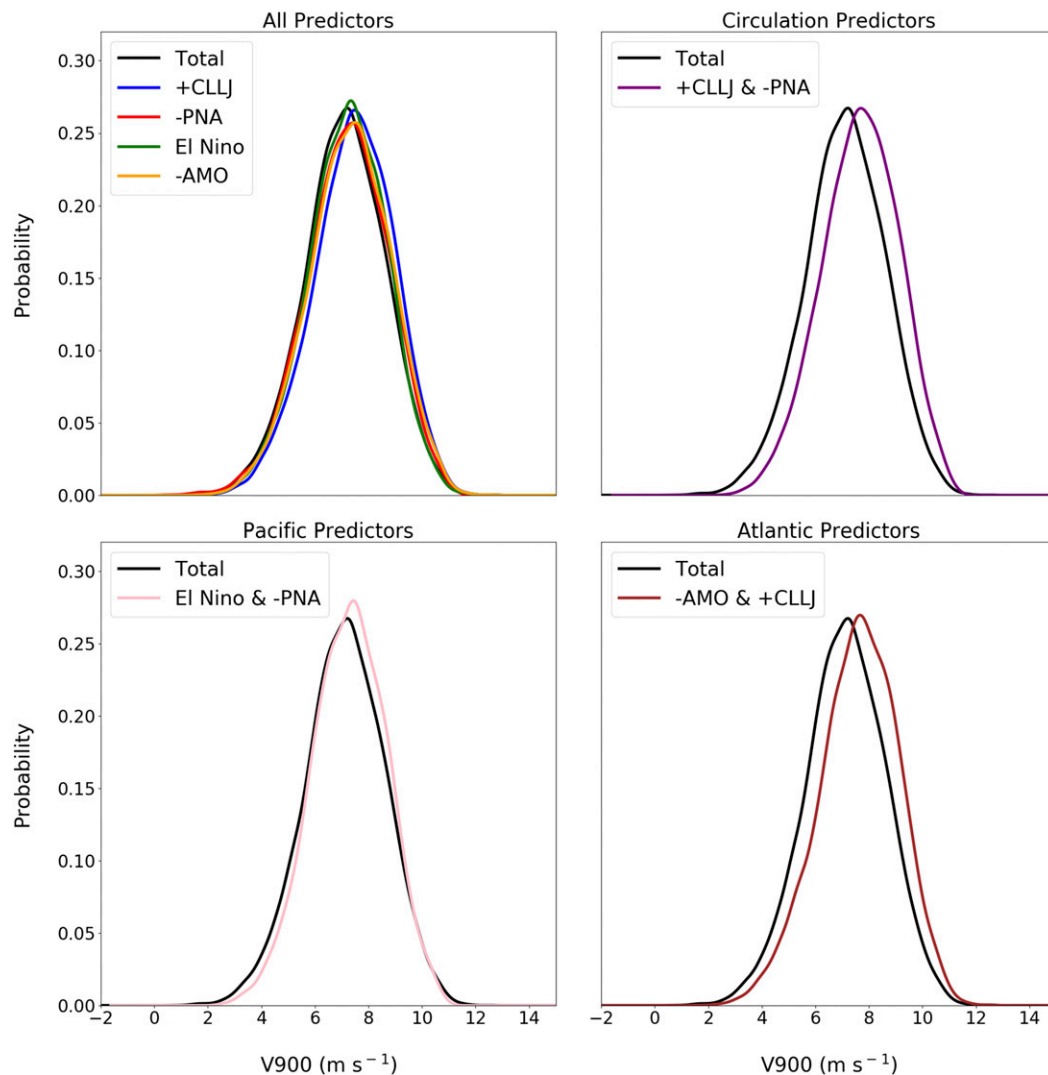


FIG. 12. As in Fig. 11, but for CCSM4.

because the model is already realistic, at least at these relatively short lead times.

Conversely, Z500 anomalies in the extratropical North Pacific and U900 anomalies in the Caribbean region show the disagreement among ensembles (Fig. 16). These circulation anomalies were plotted to analyze a pattern represented by the PNA and Caribbean LLJ, respectively. In the good forecasts, CCSM4 does not replicate the wave pattern seen in MERRA-2. There is more of a north–south dipole of Z500 stretched over the extratropical North Pacific, and perhaps the only agreement with MERRA-2 is the strong troughing over the western United States. The hatched regions suggest strong agreement among the ensembles. The bad forecasts also fail to produce the wave pattern seen in

MERRA-2. Yet, unlike the good forecasts, there is a lack of agreement in the ensembles, especially over the western United States. This suggests that high confidence of troughing over the western United States provides a forecast of opportunity. The U900 anomalies additionally present a forecast of opportunity. The good forecasts simulate the easterlies in the Caribbean, comparable to MERRA-2, and there is general ensemble agreement within the Caribbean LLJ index domain. The bad forecasts do not resemble MERRA-2, but there are unhatched regions in the Caribbean LLJ index domain for 1988 as well as for the southeastern Caribbean Sea in both 1988 and 2016. The ensembles disagree on the moisture transport from the tropical Atlantic into the Caribbean. Accordingly, the confidence for those

Case Study V900 Anomalies

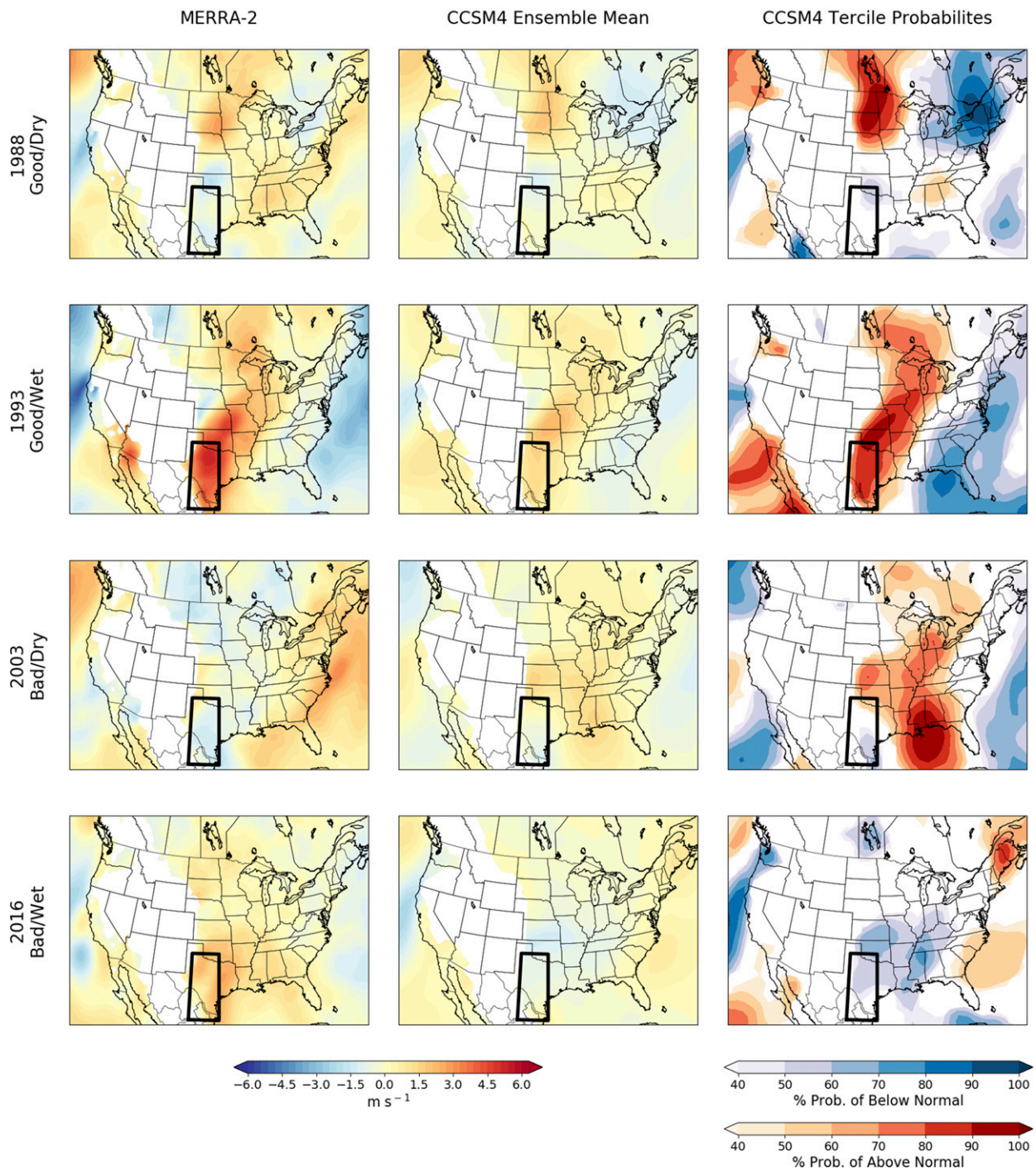


FIG. 13. V900 anomalies for (left) MERRA-2 and (center) and CCSM4 ensemble mean. (right) CCSM4 probabilities for above-normal (upper tercile) and below-normal (lower tercile) events, only showing 50% or greater probabilities. Rows indicate different case study events. Boxes indicate LLJ index domain.

Case Study Precipitation Anomalies

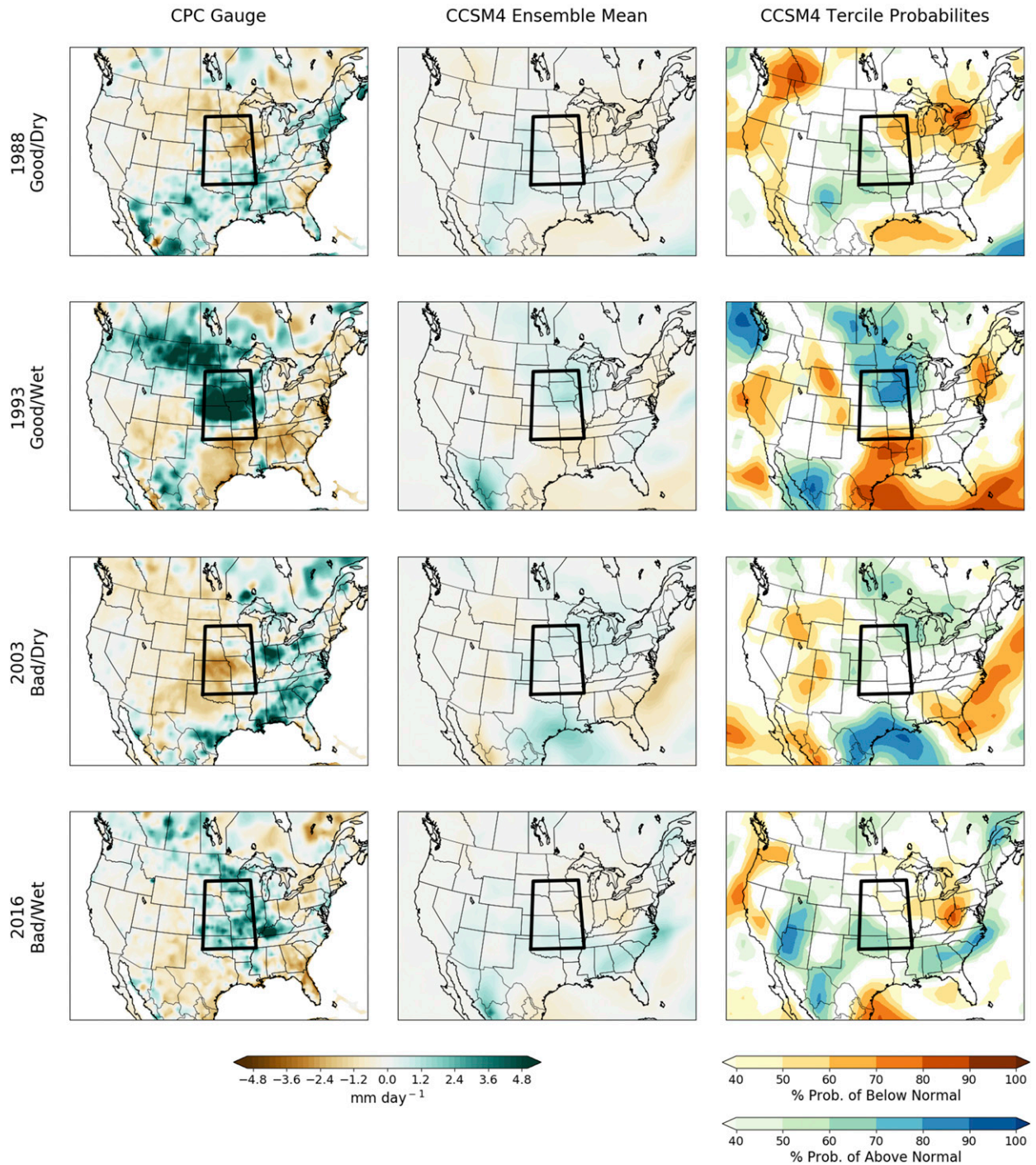


FIG. 14. As in Fig. 13, but for precipitation anomalies. Left column observations are from CPC unified gauge-based analysis. Boxes indicate Great Plains precipitation index domain.

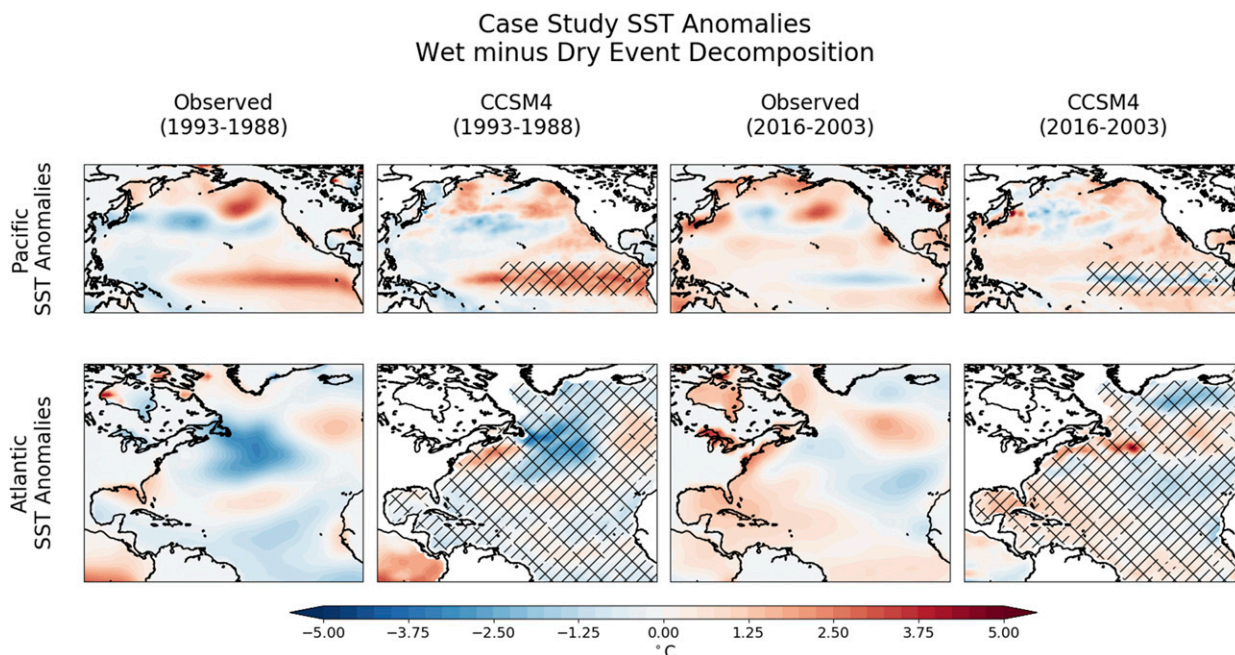


FIG. 15. Difference of SST anomalies between wet and dry events. (top) Pacific SST anomalies (color-shaded contours) as such: (left) wet event minus dry event for good forecast years in MERRA-2 (1993–88), (left center) good CCSM4 wet forecast minus good CCSM4 dry forecast (1993–88), (right center) wet event minus dry event for bad forecast years in MERRA-2 (2016–03), and (right) bad CCSM4 wet forecast minus bad CCSM4 dry forecast (2016–03). (bottom) As in the top row, but for Atlantic SST anomalies. Forward (back) hatched region describes where 70% of the ensembles agree with the sign of ensemble mean in a respective dry (wet) event, for the respective Niño-3.4 and AMO index domain.

forecasts should decrease since this is an important facilitator for Great Plains LLJ formation.

The average Z500 signal-to-noise ratios are relatively high in the western United States in MERRA-2, though CCSM4 presents low signal-to-noise ratios across the extratropical North Pacific basin and western North America (Fig. 17, top row). The average U900 signal-to-noise ratios are relatively high in the lower-left part of the Caribbean LLJ index domain in MERRA-2 and within most of the Caribbean LLJ index domain in CCSM4 (bottom row). This provides evidence that the phase of PNA and Caribbean LLJ teleconnections may present a signal beyond two weeks and aid in mid-summer subseasonal forecasting, but currently CCSM4 only hints at long-term prediction potential for the Caribbean LLJ.

4. Summary and discussion

Here we analyzed the 1982–2016 July months in MERRA-2 and CCSM4 to assess the ability of probabilistic forecasts to depict the Great Plains LLJ during this peak time for moisture fluxes and precipitation. Subseasonal forecasting of southerly LLJs starts with understanding its interannual variability in observations

and analyzing the limits of the model being employed. This study was able to evaluate the strengths and weaknesses of the CCSM4 forecasts, and it identified potential sources of predictability in the model for the Great Plains LLJ and its associated precipitation.

The CCSM4 forecasts overall overestimated the magnitude of the climatological Great Plains LLJ, extended it too far east, and misrepresented its variability. Accordingly, the magnitude of the climatological precipitation in the Great Plains and Midwest is underestimated. This forecast climatology is improved over the free-running (noninitialized) CCSM4 climatology for both V900 and precipitation. The anomaly correlation coefficient and RPSS for the forecasts revealed that the model skill for V900 decreased east of the climatological jet, and its skill for precipitation decreased outside the expected jet exit region. These regions of high anomaly correlation coefficient and RPSS are relatively consistent with NMME forecasts found on CPC website (<https://www.cpc.ncep.noaa.gov/products/NMME/>) and with Becker et al. (2014). July forecasts initialized on 1 June were also briefly investigated, addressing whether the CCSM4 forecast model has an adjustment period. In some cases, longer lead times can increase forecast skill,

Case Study Z500 and U900
Wet minus Dry Event Decomposition

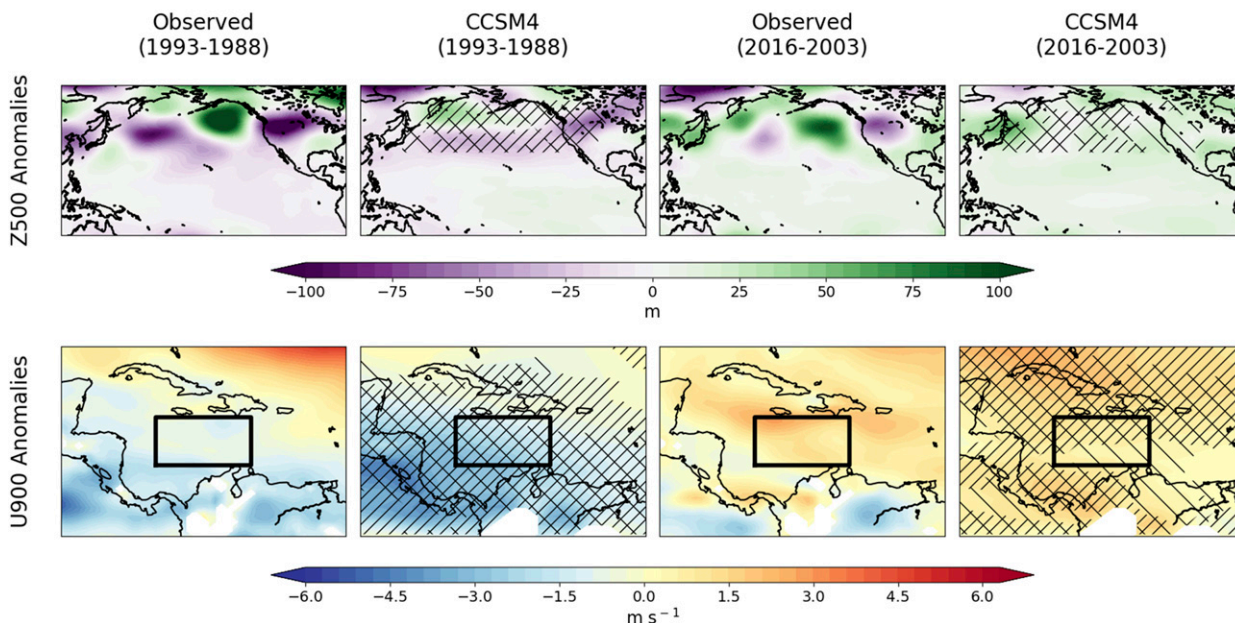


FIG. 16. As in Fig. 15, but for (top) Z500 anomalies and (bottom) U900 anomalies. Boxes indicate Caribbean LLJ index domain. Forward (back) hatched region describes where 70% of the ensembles agree with the sign of ensemble mean in a respective dry (wet) event, for the respective extratropical Pacific and entire Caribbean domain.

as the model may experience an initialization shock that reduces near-term forecast skill. The anomaly correlation coefficient and RPSS for 1 June initialization time were very low, excluding it from further analysis.

There are relationships established in the literature connecting the Great Plains LLJ to SST and circulation variability that have been explored in this study as potentially consistent predictors for the Great Plains

Average Signal-to-noise Ratios in July Monthly Means

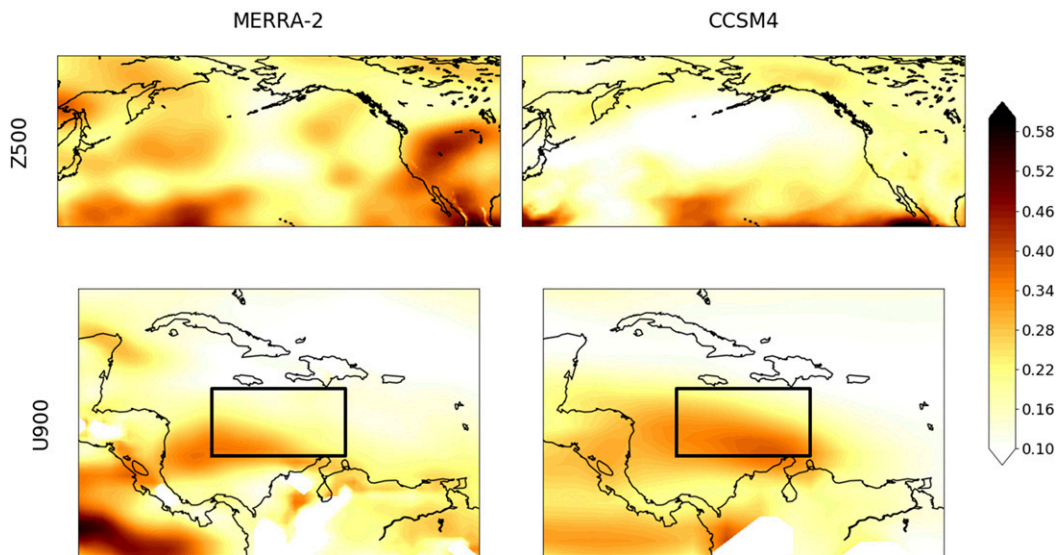


FIG. 17. Average signal-to-noise ratios in July monthly means for Z500 in (top left) MERRA-2 and (top right) CCSM4. (bottom) As in the top row, but for U900. Boxes indicate Caribbean LLJ index domain.

LLJ. MERRA-2 and CCSM4 forecasts indicate that the following features/patterns are linked to a strengthened Great Plains LLJ: 1) strong Caribbean LLJ, 2) negative PNA phase, 3) El Niño phase, and 4) cool AMO phase. The linear regressions, KDEs, and case studies suggest that perhaps the largest of forecast of opportunity is revealed through circulation predictors. CCSM4's circulation response from the Caribbean LLJ and PNA are comparable to MERRA-2, even outside the LLJ region. The KDE for positive Caribbean LLJ and negative PNA events had a large shift in MERRA-2 and CCSM4. CCSM4 forecasts failed to reproduce realistic meridional wind responses to SST anomalies outside the LLJ region. This may explain the flawed circulation forecasts (and as an extension, precipitation forecasts) in the Southeast United States.

The case study analysis decomposed the large-scale environment between good and bad forecasts. The good forecasts captured troughing over the United States and easterlies in the Caribbean Sea with an ensemble agreement of 70% or greater, suggesting that the circulation predictors (negative PNA and positive Caribbean LLJ) can be used to determine forecast confidence in CCSM4 forecasts (i.e., forecast of opportunity). In the bad forecasts, the CCSM4 ensembles lacked agreement for either one or both years. Furthermore, the MERRA-2 signal-to-noise ratios for the Z500 July monthly mean were highest in the western United States, and the ratios for the U900 July monthly mean were highest in the Caribbean Sea, supporting that these circulation predictors may hold influence beyond two weeks. However, CCSM4 only exhibits the high signal-to-noise ratios for U900 in the Caribbean Sea. Interestingly, the PNA pattern was a persistent signal in MERRA-2 for both cases, and the CCSM4 was confident in its incorrect circulation over the extratropical North Pacific. This highlights that PNA-like wave excitation is not always forced by ENSO alone (Ding et al. 2011; Zhu and Li 2016), and the model may fail to represent variability in the extratropical North Pacific (Fig. 17), which should be explored in future studies.

Results from Kam et al. (2014) are consistent with our interpretation of SST anomalies in subseasonal mid-summer climate forecasting. Confidence in the forecast should depend less on the phase of ENSO and AMO. They argued that the link between Midwest hydroclimate and SST anomalies is strongly coupled in the NMME climate forecast models and may overestimate their relationship and negatively affect skill. This is analogous to the case study forecast for 2016 (bad/wet), which had a cooler signal in the equatorial Pacific and warmer signal in the Atlantic (Fig. 15, columns 3 and 4)

that could explain a poor forecast of dry anomalies in the Midwest (Fig. 14, bottom row).

Generally, there are shortcomings when using only four cases to demonstrate the complexity of SST and circulation variability. These cases are not representative of all extreme wet and dry months. Instead, they are merely used to help explain discrepancies in these bad forecasts and find consistent patterns of model agreement in the good forecasts. Using monthly means only considers contemporaneous links between the Great Plains LLJ and precipitation as well as the predictor and Great Plains LLJ. Lead-lag relationships exist between the Great Plains LLJ and precipitation (Weaver and Nigam 2011), ENSO (Danco and Martin 2018; Krishnamurthy et al. 2015), PNA (Harding and Snyder 2015), and Caribbean LLJ (Krishnamurthy et al. 2015). Last, dry months are not necessarily equal and opposite manifestations of the circulation in wet months.

Future research will need to address the differences between spring and late-summer Great Plains LLJ variability and mechanisms. Interannual SST variability still has several unanswered questions, such as whether seasonal transition of El Niño affects the jet or if the tropical Atlantic has a role. CCSM4 should be explored for how it depicts topography modulation and associated Great Plains LLJ formation. In addition, there are potentially other factors to consider as predictors, such as sea surface salinity over subtropical North Atlantic (Li et al. 2016; Li et al. 2017) and low-level vorticity over the Southeast United States (Pu et al. 2016). Soil moisture is a significant predictor of Great Plains LLJ and Great Plains precipitation that was not discussed. It has not been overlooked, but rather CCSM4 is recognized as having low land-atmosphere coupling (Infanti and Kirtman 2016). Atmospheric initialization has been shown to be a much stronger influence than land initialization on precipitation (and temperature) prediction on sub-seasonal time scales.

Accurate subseasonal and seasonal prediction of the Great Plains LLJ and precipitation is still distant. There are hurdles to overcome in many models' representations of them; nevertheless, any advancement toward forecasting heavy precipitation events with greater lead time is certainly valuable.

Acknowledgments. The authors acknowledge support from NOAA NA15OAR4320064, NA16OAR4310141, NA16OAR4310149, and NA18OAR4310293. The University of Miami Center for Computational Science (CCS) provided the computational resources to complete the numerical experiments, and the authors are

most grateful for the use of the Community Climate System Model from NCAR. Last, the authors want to thank Dr. Gary Lackmann and two anonymous reviewers for their thoughtful and thorough feedback on the manuscript, which greatly improved its structure and content.

REFERENCES

- Arritt, R. W., T. D. Rink, M. Segal, D. P. Todey, C. A. Clark, M. J. Mitchell, and K. M. Labas, 1997: The Great Plains low-level jet during the warm season of 1993. *Mon. Wea. Rev.*, **125**, 2176–2192, [https://doi.org/10.1175/1520-0493\(1997\)125<2176:TGPLLJ>2.0.CO;2](https://doi.org/10.1175/1520-0493(1997)125<2176:TGPLLJ>2.0.CO;2).
- Banta, R., R. K. Newsom, J. K. Lundquist, Y. L. Pichugina, R. L. Coulter, and L. Mahrt, 2002: Nocturnal low-level jet characteristics over Kansas during CASES-99. *Bound.-Layer Meteor.*, **105**, 221–252, <https://doi.org/10.1023/A:1019992330866>.
- Barnston, A. G., and R. E. Livezey, 1987: Classification, seasonality and persistence of low-frequency atmospheric circulation patterns. *Mon. Wea. Rev.*, **115**, 1083–1126, [https://doi.org/10.1175/1520-0493\(1987\)115<1083:CSAPOL>2.0.CO;2](https://doi.org/10.1175/1520-0493(1987)115<1083:CSAPOL>2.0.CO;2).
- Becker, E., H. den Dool, and Q. Zhang, 2014: Predictability and forecast skill in NMME. *J. Climate*, **27**, 5891–5906, <https://doi.org/10.1175/JCLI-D-13-00597.1>.
- Blackadar, A. K., 1957: Boundary layer wind maxima and their significance for the growth of nocturnal inversions. *Bull. Amer. Meteor. Soc.*, **38**, 283–290, <https://doi.org/10.1175/1520-0477-38.5.283>.
- Bosilovich, M. G., and Coauthors, 2015: MERRA-2: Initial evaluation of the climate. NASA Tech. Memo. NASA/TM-2015-104606/Vol. 43, NASA, 145 pp.
- Byerle, L. A., and J. Paegle, 2003: Modulation of the Great Plains low-level jet and moisture transports by orography and large-scale circulations. *J. Geophys. Res.*, **108**, 8611, <https://doi.org/10.1029/2002JD003005>.
- Chen, M., W. Shi, P. Xie, V. B. S. Silva, V. E. Kousky, R. Wayne Higgins, and J. E. Janowiak, 2008: Assessing objective techniques for gauge-based analyses of global daily precipitation. *J. Geophys. Res.*, **113**, D04110, <https://doi.org/10.1029/2007JD009132>.
- Cook, K. H., E. K. Vizi, Z. S. Launer, and C. M. Patricola, 2008: Springtime intensification of the Great Plains low-level jet and Midwest precipitation in GCM simulations of the twenty-first century. *J. Climate*, **21**, 6321–6340, <https://doi.org/10.1175/2008JCLI2355.1>.
- Danco, J. F., and E. R. Martin, 2018: Understanding the influence of ENSO on the Great Plains low-level jet in CMIP5 models. *Climate Dyn.*, **51**, 1537–1558, <https://doi.org/10.1007/s00382-017-3970-9>.
- Ding, Q., B. Wang, J. M. Wallace, and G. Branstator, 2011: Tropical–extratropical teleconnections in boreal summer: Observed interannual variability. *J. Climate*, **24**, 1878–1896, <https://doi.org/10.1175/2011JCLI3621.1>.
- Dirmeyer, P. A., and J. L. Kinter, 2010: Floods over the U.S. Midwest: A regional water cycle perspective. *J. Hydrometeor.*, **11**, 1172–1181, <https://doi.org/10.1175/2010JHM1196.1>.
- Fast, J. D., and M. D. McCorcle, 1990: A two-dimensional numerical sensitivity study of the Great Plains low-level jet. *Mon. Wea. Rev.*, **118**, 151–164, [https://doi.org/10.1175/1520-0493\(1990\)118<0151:ATDNSS>2.0.CO;2](https://doi.org/10.1175/1520-0493(1990)118<0151:ATDNSS>2.0.CO;2).
- Feldstein, S. B., 2000: The timescale, power spectra, and climate noise properties of teleconnection patterns. *J. Climate*, **13**, 4430–4440, [https://doi.org/10.1175/1520-0442\(2000\)013<4430:TTPSAC>2.0.CO;2](https://doi.org/10.1175/1520-0442(2000)013<4430:TTPSAC>2.0.CO;2).
- Feng, Z., L. R. Leung, S. Hagos, R. A. Houze, C. D. Burleyson, and K. Balaguru, 2016: More frequent intense and long-lived storms dominate the springtime trend in central US rainfall. *Nat. Commun.*, **7**, 13 429, <https://doi.org/10.1038/ncomms13429>.
- Gelaro, R., and Coauthors, 2017: The Modern-Era Retrospective Analysis for Research and Applications, version 2 (MERRA-2). *J. Climate*, **30**, 5419–5454, <https://doi.org/10.1175/JCLI-D-16-0758.1>.
- Gimeno, L., and Coauthors, 2016: Major mechanisms of atmospheric moisture transport and their role in extreme precipitation events. *Annu. Rev. Environ. Resour.*, **41**, 117–141, <https://doi.org/10.1146/annurev-environ-110615-085558>.
- Harding, K. J., and P. K. Snyder, 2015: The relationship between the Pacific–North American teleconnection pattern, the Great Plains low-level jet, and north-central U.S. heavy rainfall events. *J. Climate*, **28**, 6729–6742, <https://doi.org/10.1175/JCLI-D-14-00657.1>.
- Higgins, R. W., Y. Yao, E. S. Yarosh, J. E. Janowiak, and K. C. Mo, 1997: Influence of the Great Plains low-level jet on summertime precipitation and moisture transport over the central United States. *J. Climate*, **10**, 481–507, [https://doi.org/10.1175/1520-0442\(1997\)010<0481:IOTGPL>2.0.CO;2](https://doi.org/10.1175/1520-0442(1997)010<0481:IOTGPL>2.0.CO;2).
- Hodges, D., and Z. Pu, 2019: Characteristics and variations of low-level jets in the contrasting warm season precipitation extremes of 2006 and 2007 over the Southern Great Plains. *Theor. Appl. Climatol.*, **136**, 753–771, <https://doi.org/10.1007/s00704-018-2492-7>.
- Holton, J. R., 1967: The diurnal boundary layer wind oscillation above sloping terrain. *Tellus*, **19A**, 200–205, <https://doi.org/10.3402/tellusa.v19i2.9766>.
- Hu, Q., and S. Feng, 2012: AMO- and ENSO-driven summertime circulation and precipitation variations in North America. *J. Climate*, **25**, 6477–6495, <https://doi.org/10.1175/JCLI-D-11-00520.1>.
- Huang, B., and Coauthors, 2017: Extended Reconstructed Sea Surface Temperature, version 5 (ERSSTv5): Upgrades, validations, and intercomparisons. *J. Climate*, **30**, 8179–8205, <https://doi.org/10.1175/JCLI-D-16-0836.1>.
- Infanti, J. M., and B. P. Kirtman, 2016: Prediction and predictability of land and atmosphere initialized CCSM4 climate forecasts over North America. *J. Geophys. Res. Atmos.*, **121**, 12 690–12 701, <https://doi.org/10.1002/2016JD024932>.
- Jiang, X., N. Lau, I. M. Held, and J. J. Ploshay, 2007: Mechanisms of the Great Plains low-level jet as simulated in an AGCM. *J. Atmos. Sci.*, **64**, 532–547, <https://doi.org/10.1175/JAS3847.1>.
- Kam, J., J. Sheffield, X. Yuan, and E. F. Wood, 2014: Did a skillful prediction of sea surface temperatures help or hinder forecasting of the 2012 Midwestern US drought? *Environ. Res. Lett.*, **9** (3), <https://doi.org/10.1088/1748-9326/9/3/034005>.
- Kirtman, B. P., and D. Min, 2009: Multimodel ensemble ENSO prediction with CCSM and CFS. *Mon. Wea. Rev.*, **137**, 2908–2930, <https://doi.org/10.1175/2009MWR2672.1>.
- , and Coauthors, 2014: The North American Multimodel Ensemble: Phase-1 seasonal-to-interannual prediction; Phase-2 toward developing intraseasonal prediction. *Bull. Amer. Meteor. Soc.*, **95**, 585–601, <https://doi.org/10.1175/BAMS-D-12-00050.1>.
- Krishnamurthy, L., G. A. Vecchi, R. Msadek, A. Wittenberg, T. L. Delworth, and F. Zeng, 2015: The seasonality of the Great Plains low-level jet and ENSO relationship. *J. Climate*, **28**, 4525–4544, <https://doi.org/10.1175/JCLI-D-14-00590.1>.

- Li, L., R. W. Schmitt, C. C. Ummenhofer, and K. B. Karnauskas, 2016: Implications of North Atlantic sea surface salinity for summer precipitation over the U.S. Midwest: Mechanisms and predictive value. *J. Climate*, **29**, 3143–3159, <https://doi.org/10.1175/JCLI-D-15-0520.1>.
- , —, and —, 2017: The role of the subtropical North Atlantic water cycle in recent US extreme precipitation events. *Climate Dyn.*, **50**, 1–15, <https://doi.org/10.1007/s00382-017-3685-y>.
- Mallakpour, I., and G. Villarini, 2016: Investigating the relationship between the frequency of flooding over the central United States and large-scale climate. *Adv. Water Resour.*, **92**, 159–171, <https://doi.org/10.1016/j.advwatres.2016.04.008>.
- Mestas-Núñez, A. M., D. B. Enfield, and C. Zhang, 2007: Water vapor fluxes over the Intra-Americas Sea: Seasonal and interannual variability and associations with rainfall. *J. Climate*, **20**, 1910–1922, <https://doi.org/10.1175/JCLI4096.1>.
- Nayak, M. A., and G. Villarini, 2017: A long-term perspective of the hydroclimatological impacts of atmospheric rivers over the central United States. *Water Resour. Res.*, **53**, 1144–1166, <https://doi.org/10.1002/2016WR019033>.
- Mitchell, M. J., R. W. Arritt, and K. Labas, 1995: A climatology of the warm season Great Plains low-level jet using wind profiler observations. *Wea. Forecasting*, **10**, 576–591, [https://doi.org/10.1175/1520-0434\(1995\)010<0576:ACOTWS>2.0.CO;2](https://doi.org/10.1175/1520-0434(1995)010<0576:ACOTWS>2.0.CO;2).
- Paolino, D. A., J. L. Kinter III, B. P. Kirtman, D. Min, and D. M. Straus, 2012: The impact of land surface initialization on seasonal forecasts with CCSM. *J. Climate*, **25**, 1007–1021, <https://doi.org/10.1175/2011JCLI3934.1>.
- Parish, T. R., and L. D. Oolman, 2010: On the role of sloping terrain in the forcing of the Great Plains low-level jet. *J. Atmos. Sci.*, **67**, 2690–2699, <https://doi.org/10.1175/2010JAS3368.1>.
- , A. R. Rodi, and R. D. Clark, 1988: A case study of the summertime Great Plains low level jet. *Mon. Wea. Rev.*, **116**, 94–105, [https://doi.org/10.1175/1520-0493\(1988\)116<0094:ACSOTS>2.0.CO;2](https://doi.org/10.1175/1520-0493(1988)116<0094:ACSOTS>2.0.CO;2).
- Patricola, C. M., P. Chang, and R. Saravanan, 2015: Impact of Atlantic SST and high frequency atmospheric variability on the 1993 and 2008 Midwest floods: Regional climate model simulations of extreme climate events. *Climatic Change*, **129**, 397–411, <https://doi.org/10.1007/s10584-013-0886-1>.
- Pu, B., and R. E. Dickinson, 2014: Diurnal spatial variability of Great Plains summer precipitation related to the dynamics of the low-level jet. *J. Atmos. Sci.*, **71**, 1807–1817, <https://doi.org/10.1175/JAS-D-13-0243.1>.
- , —, and R. Fu, 2016: Dynamical connection between Great Plains low-level winds and variability of central Gulf States precipitation. *J. Geophys. Res. Atmos.*, **121**, 3421–3434, <https://doi.org/10.1002/2015JD024045>.
- Shapiro, A., E. Fedorovich, and S. Rahimi, 2016: A unified theory for the Great Plains nocturnal low-level jet. *J. Atmos. Sci.*, **73**, 3037–3057, <https://doi.org/10.1175/JAS-D-15-0307.1>.
- Simmons, A. J., R. Mureau, and T. Petroliaigis, 1995: Error growth and estimates of predictability from the ECMWF forecasting system. *Quart. J. Roy. Meteor. Soc.*, **121**, 1739–1771, <https://doi.org/10.1002/qj.49712152711>.
- Ting, M., and H. Wang, 1997: Summertime U.S. precipitation variability and its relation to Pacific sea surface temperature. *J. Climate*, **10**, 1853–1873, [https://doi.org/10.1175/1520-0442\(1997\)010<1853:SUSPVA>2.0.CO;2](https://doi.org/10.1175/1520-0442(1997)010<1853:SUSPVA>2.0.CO;2).
- , and —, 2006: The role of the North American topography on the maintenance of the Great Plains summer low-level jet. *J. Atmos. Sci.*, **63**, 1056–1068, <https://doi.org/10.1175/JAS3664.1>.
- Trenberth, K. E., and C. J. Guillemot, 1996: Physical processes involved in the 1988 drought and 1993 floods in North America. *J. Climate*, **9**, 1288–1298, [https://doi.org/10.1175/1520-0442\(1996\)009<1288:PPIITD>2.0.CO;2](https://doi.org/10.1175/1520-0442(1996)009<1288:PPIITD>2.0.CO;2).
- Veres, M. C., and Q. Hu, 2013: AMO-forced regional processes affecting summertime precipitation variations in the central United States. *J. Climate*, **26**, 276–290, <https://doi.org/10.1175/JCLI-D-11-00670.1>.
- Wang, C., 2007: Variability of the Caribbean low-level jet and its relations to climate. *Climate Dyn.*, **29**, 411–422, <https://doi.org/10.1007/s00382-007-0243-z>.
- Weaver, S. J., 2013: Factors associated with decadal variability in Great Plains summertime surface temperatures. *J. Climate*, **26**, 343–350, <https://doi.org/10.1175/JCLI-D-11-00713.1>.
- , and S. Nigam, 2008: Variability of the Great Plains low-level jet: Large-scale circulation context and hydroclimate impacts. *J. Climate*, **21**, 1532–1551, <https://doi.org/10.1175/2007JCLI1586.1>.
- , and —, 2011: Recurrent supersynoptic evolution of the Great Plains low-level jet. *J. Climate*, **24**, 575–582, <https://doi.org/10.1175/2010JCLI3445.1>.
- , A. Ruiz-Barradas, and S. Nigam, 2009a: Pentad evolution of the 1988 drought and 1993 flood over the Great Plains: An NARR perspective on the atmospheric and terrestrial water balance. *J. Climate*, **22**, 5366–5384, <https://doi.org/10.1175/2009JCLI2684.1>.
- , S. Schubert, and H. Wang, 2009b: Warm season variations in the low-level circulation and precipitation over the central United States in observations, AMIP simulations, and idealized SST experiments. *J. Climate*, **22**, 5401–5420, <https://doi.org/10.1175/2009JCLI2984.1>.
- , S. Baxter, and K. Harnos, 2016: Regional changes in the interannual variability of U.S. warm season precipitation. *J. Climate*, **29**, 5157–5173, <https://doi.org/10.1175/JCLI-D-14-00803.1>.
- Weigel, A. P., M. A. Liniger, and C. Appenzeller, 2007: The discrete Brier and ranked probability skill scores. *Mon. Wea. Rev.*, **135**, 118–124, <https://doi.org/10.1175/MWR3280.1>.
- Whiteman, C. D., X. Bian, and S. Zhong, 1997: Low-level jet climatology from enhanced rawinsonde observations at a site in the Southern Great Plains. *J. Appl. Meteor.*, **36**, 1363–1376, [https://doi.org/10.1175/1520-0450\(1997\)036<1363:LLJCFE>2.0.CO;2](https://doi.org/10.1175/1520-0450(1997)036<1363:LLJCFE>2.0.CO;2).
- Wilks, D. S., 1995: *Statistical Methods in the Atmospheric Sciences: An Introduction*. International Geophysics Series, Vol. 59, Elsevier, 467 pp.
- Xie, P., M. Chen, S. Yang, A. Yatagai, T. Hayasaka, Y. Fukushima, and C. Liu, 2007: A gauge-based analysis of daily precipitation over East Asia. *J. Hydrometeorol.*, **8**, 607–626, <https://doi.org/10.1175/JHM583.1>.
- Yu, L., S. Zhong, W. E. Heilman, and X. Bian, 2016: The effect of two types of El Niño on the southerly low-level jets in North America. *Earth Space Sci.*, **3**, 306–317, <https://doi.org/10.1002/2016EA000164>.
- , —, J. A. Winkler, D. L. Doubler, X. Bian, and C. K. Walters, 2017: The inter-annual variability of southerly low-level jets in North America. *Int. J. Climatol.*, **37**, 343–357, <https://doi.org/10.1002/joc.4708>.
- Zhu, Z., and T. Li, 2016: A new paradigm for continental U.S. summer rainfall variability: Asia–North America teleconnection. *J. Climate*, **29**, 7313–7327, <https://doi.org/10.1175/JCLI-D-16-0137.1>.